

Summer 2019

Development of an Automated Fiber Placement Process for the Fabrication of Thermoplastic Composite Laminates

Anthony M. Sabido

Follow this and additional works at: <https://scholarcommons.sc.edu/etd>



Part of the [Aerospace Engineering Commons](#)

Recommended Citation

Sabido, A. M.(2019). *Development of an Automated Fiber Placement Process for the Fabrication of Thermoplastic Composite Laminates*. (Master's thesis). Retrieved from <https://scholarcommons.sc.edu/etd/5332>

This Open Access Thesis is brought to you by Scholar Commons. It has been accepted for inclusion in Theses and Dissertations by an authorized administrator of Scholar Commons. For more information, please contact digres@mailbox.sc.edu.

DEVELOPMENT OF AN AUTOMATED FIBER PLACEMENT PROCESS FOR THE
FABRICATION OF THERMOPLASTIC COMPOSITE LAMINATES

by

Anthony M. Sabido

Bachelor of Science
Florida State University, 2012

Submitted in Partial Fulfillment of the Requirements

For the Degree of Master of Science in

Aerospace Engineering

College of Engineering and Computing

University of South Carolina

2019

Accepted by:

Michel Van Tooren, Director of Thesis

Ramy Harik, Reader

Cheryl L. Addy, Vice Provost and Dean of the Graduate School

© Copyright by Anthony M. Sabido, 2019
All Rights Reserved.

ACKNOWLEDGEMENTS

I would like to thank Andrew Eulberg, Michael Keifer, Burton Rhodes, Susan Rogers, Rachael Rudd, and Tyler Strampp for all of their assistance and expertise. I could not have asked for better Team Wombat members to have helped me along the way. I would also like to thank my advisors Dr. Michel Van Tooren and Dr. Ramy Harik. Without their support and assistance, I would not have finished my graduate career at the University of South Carolina. Lastly, I would like to thank my parents Jorge and Marisol Sabido. Their love and support have always aided me in tackling any challenges in my path.

ABSTRACT

An automated fiber placement process is desired for manufacturing variable-stiffness thermoplastic composite laminates. By developing such a composite laminate, it is possible to take advantage of the tunable performance increases that are achievable by spatially steering individual tows. In addition, using a thermoplastic polymer as the matrix material has many advantages: a high toughness, ability to employ thermoplastic joining processes that do not require adhesives, long storage life, and lacks the need to be refrigerated. This process was experimentally developed, where the effect of various process parameters on the quality of the laminate were evaluated. An experimental AFP head was developed in order to monitor and record the compaction pressure, heating temperature, tool temperature, and tow tension in-situ. By comparing the resulting layups to traditional processes, a quantitative assessment is made on the ability to automatically place thermoplastic composite tows for the manufacturing of constant stiffness composite laminates. Lastly, the feasibility of utilizing this process for the fabrication of variable stiffness thermoplastic composites is assessed.

TABLE OF CONTENTS

ACKNOWLEDGEMENTS	iii
ABSTRACT	iv
LIST OF TABLES	viii
LIST OF FIGURES	x
LIST OF SYMBOLS	xii
LIST OF ABBREVIATIONS.....	xiv
CHAPTER 1 INTRODUCTION	1
CHAPTER 2 LITERATURE REVIEW	4
2.1 EARLY DEVELOPMENTS.....	4
2.2 MANUFACTURING CONSTRAINTS	6
2.3 TOOL PATH DESIGN	10
2.4 THERMOPLASTIC COMPOSITES	12
CHAPTER 3 RESEARCH OBJECTIVES.....	15
3.1 MATERIAL SELECTION	16
3.2 AUTOMATED FIBER PLACEMENT	19
3.3 PROCESS EVALUATION.....	24

CHAPTER 4 EXPERIMENTAL PROCEDURES.....	25
4.1 DESIGN OF EXPERIMENTS.....	25
4.2 TENSILE TESTING.....	36
4.3 DRYING OF CARBON/PEI TOWS	39
CHAPTER 5 PRELIMINARY EXPERIMENTAL SETUP	41
5.1 OVERVIEW.....	41
5.2 FIBER PLACEMENT HEAD	43
5.3 HEAT SOURCES	45
5.4 FIBER TENSIONER	47
5.5 HEATED TOOL.....	49
5.6 INTEGRATION WITH ARTICULATED ROBOT ARM.....	50
CHAPTER 6 RESULTS AND ANALYSIS.....	53
6.1 HEAT SOURCE COMPARISON	53
6.2 HEATING LIMITATIONS	58
6.3 COMPACTION PRESSURE.....	60
6.4 TOW TENSION.....	69
6.5 FEED RATE AND PLY NUMBER	69
6.6 LAMINATE MANUFACTURING CHALLENGES.....	71
6.7 FIBER STEERING	74
CHAPTER 7 CONCLUSIONS	76

CHAPTER 8 FUTURE WORK AND RECOMMENDATIONS	79
REFERENCES	82

LIST OF TABLES

Table 3.1 Typical Mechanical Properties for Cetex TC1000 (PEI), AS4, 145gsm, 32% RC	16
Table 3.2 Typical Material Properties for ULTEM™ Resin 1000	16
Table 3.3 Typical Material Properties for HexTow® AS4 6K Carbon Fiber	17
Table 3.4 Process Variables	20
Table 3.5 Experiment Descriptions	21
Table 4.1 Control Factors for Experiment 1	26
Table 4.2 Full Factorial Design for Experiment 1	27
Table 4.3 Baseline Process Parameters for Experiment 2	28
Table 4.4 Control Factors for Experiment 2	29
Table 4.5 Orthogonal Array $L_9(3^4)$ for Experiment 2	29
Table 4.6 Control Factors for Experiment 3	30
Table 4.7 Orthogonal Array $L_9(3^3)$ for Experiment 3	31
Table 4.8 Control Factors for Experiment 4	32
Table 4.9 Control Factors for Experiment 5a ($n = 3$)	33
Table 4.10 Control Factors for Experiment 5b ($n = 5$)	33
Table 4.11 Control Factors for Experiment 5c ($n = 7$)	34
Table 4.12 Full Factorial Design for Experiment 5	34
Table 6.1 Material Temperatures Reached for $h_1 = 10$ mm and $h_2 = 15$ mm	53

Table 6.2 Compaction pressure at each of the rollers (MPa).....	60
Table 6.3 Optimum Compaction Force vs. Number of Rollers.....	61
Table 6.4 SLS Test Results for Experiment 4.....	67
Table 6.5 SLS Test Results for Control Specimens.....	67
Table 6.6 Results for Experiment 5	69

LIST OF FIGURES

Figure 1.1 Schematic of an ATL head (left) [1] and an AFP head (right) [2]	4
Figure 3.1 Experimental AFP Machine	19
Figure 4.1 Feasible roller speeds for each layer during a 20-ply lay-up process with a preheat temperature of 150 °C [3].	35
Figure 4.2 Single Lap Shear Specimen with [0/0] Orientation.....	36
Figure 4.3 Control Specimens.....	38
Figure 5.1 AFP Design Flow Chart	41
Figure 5.2 AFP Head with 4 Roller Setup	42
Figure 5.3 AFP Head Cross-Section with Dimensions.....	43
Figure 5.4 Compaction Force vs. Roller Displacement.....	44
Figure 5.5 303D Hot Air Rework Station and Modified Heater Tip	45
Figure 5.6 T835 Solder Station.....	46
Figure 5.7 Repositionable Spool with Drag Braking System	47
Figure 5.8 Mechanical Tensioner with Fitted Force Gage	48
Figure 5.9 Heated Tool and PID Controller Setup	49
Figure 5.10 EtherCAT Fieldbus System and Power Supply.....	50
Figure 6.1 Average Material Temperature vs. HA Heater Temperature Setting.....	53
Figure 6.2 Material temperature as a function of time for $h = 10mm$	54
Figure 6.3 IR heating over time with $h = 5 mm, T_t = 150 °C$	56

Figure 6.4 Secondary and Primary Heater Positioning.....	58
Figure 6.5 Normal Stress for Primary Roller vs. Compaction Force ($N_r = 4$).....	62
Figure 6.6 Normal Stress for Secondary Rollers vs. Compaction Force ($N_r = 4$)	63
Figure 6.7 Shear Stress Distributions for Various Compaction Forces	64
Figure 6.8 Contact Width and Normal Stress vs. Roller Diameter.....	65
Figure 6.9 Layup on 3 layers ($n = 3$) at $f = 3 \text{ mm/s}$ (left) and $f = 2.5 \text{ mm/s}$ (right).....	69
Figure 6.10 In-situ consolidation challenges during the layup of the 3 rd layer.....	72
Figure 6.11 Fiber steering trials at a radius of 200 mm	74
Figure 8.1 Second prototype for a thermoplastic AFP machine	79

LIST OF SYMBOLS

H	Heat Source being used for primary heating of the tow being placed.
h	Distance of the heat source to the tool surface.
T_t	Temperature of the tool being consolidated on by the automated fiber placement head.
T_h	Temperature setting of the primary heater.
T_{AFP}	Temperature setting of the secondary heater used to increase the overall temperature of the compaction roller and heated zone.
T	Temperature reached by the consolidated material being heated.
T_{avg}	Average temperature reached by the consolidated material being heated.
T_{max}	Maximum temperature reached by the consolidated material being heated.
t_{ss}	Time until a steady state temperature is reached by the consolidated material being heated.
f	Feed rate reached by the tool, equivalent to the roller speed for robot mounted automated fiber placement heads.
F_t	Tow tension set by the unidirectional drag braking system on the spool.
F_c	Compaction force caused by the compression of the automated fiber placement head by the robot mounted tool.
N_r	Total number of rollers used, consisting of 1 primary compaction roller and several secondary rollers.
n	Number of layers that have been consolidated on the tool.
L	Length of overlap by 2 tows where they will be bonded together.
t	Thickness of the tow being consolidated.

- F_{ty} Tensile strength of the tow.
- τ Average shear strength
- b The half width of the contact area between a cylindrical roller and a surface.
- K_b A dependent variable used in Hertzian Contact Theory for the analysis of two cylindrical rollers in contact with parallel axis.
- ν Poisson's ratio.
- E Elastic modulus.
- d Diameter of the cylinder(s) used in the Hertzian contact stress formulations.

LIST OF ABBREVIATIONS

AFP	Automated Fiber Placement
AFS	Automated Fiber Steering
ATL	Automated Tape Layup
CA	Cellular Automata
DAO	Domain of Admissible Orientation
DOE	Design of Experiments
FW	Filament Winding
HA	Hot Air
IR	Infrared
LP	Lamination Parameters
NOL	Naval Ordnance Laboratory
PEEK	Polyetheretherketone
PEI	Polyetherimide
PEKK	Polyetherketoneketone
PPS	Polyphenylene Sulfide
VSC	Variable Stiffness Composites

CHAPTER 1 INTRODUCTION

While Hyer and Charette have explored the optimization of fiber directions throughout the domain of a VSC as early as 1987 [4], research on manufacturing processes for such a composite laminate is a comparatively young area of study. In the context of this paper, composite materials consist of a fibrous load bearing material embedded in a resin matrix. By developing constituent materials for a composite, it is possible to design a material that has a resultant set of properties tailored for a specific structural purpose. Early research focused on improving the constituent materials by developing high stiffness fibers, such as carbon/graphite, and high performance polymer resins. Laminate design typically consists of determining the optimum materials, constituent volume fraction, and ply stacking sequence where the resulting properties are anisotropic. By orienting the fibers spatially within each ply, we expand and optimize the laminate design space. The fiber paths in VSC can be tailored to maximize one or several objective functions, such as minimum compliance or maximum strength. This is a challenging concept to implement due to computing, monetary, and manufacturing constraints. By allowing the fiber direction and volume fractions to be treated as design variables, the computational requirements to optimize the laminate design increase substantially. In addition, manufacturing a laminate where the fibers are tailored is extremely labor intensive. The equipment needed to design and fabricate these composite

materials increase the overall costs associated with implementing VSC into various industries.

The use of thermoplastic polymers as a matrix material in VSC is essentially nonexistent. In the aerospace industry, thermoset polymers are much more prevalent than expensive thermoplastics. Thermoplastics (PPS, PEI, PEEK, PEKK, etc.) have several characteristics that make them desirable for use in the aerospace composites. Due to the cross-linking that occurs in curing thermosets, thermoplastic composites generally exhibit greater impact resistance and damage tolerance. There is also a benefit in the handling and storage of thermoplastics, when compared to thermosets. Thermosets, for example, require storage under refrigeration and have a much shorter shelf life. Comparatively, thermoplastics have a near infinite shelf life and do not require refrigeration.

Thermoplastics do absorb moisture during storage, however, negatively affecting the material's performance. Sharp, Holmes, and Woodall showed the moisture absorption for AS4/APC-2 (Carbon/PEEK) specimens and identified a saturation of 0.20% after 130 days [5]. It is therefore often necessary to include an additional prep-processing step of using a drying unit to remove the moisture. While thermoplastic composites being manufactured using automated fiber placement certainly isn't new, the introduction of fiber steering introduces several challenges that have yet to be thoroughly addressed.

In order to achieve the goal of fiber steering thermoplastic composites, this research aims to develop an AFP process for manufacturing thermoplastic composites and determine the viability of steering thermoplastic composite tows. In order to accomplish this, many of the challenges of using a thermoplastic composite material must be addressed by developing a unique experimental tool. One of the main challenges includes

the relatively high stiffness of the tows (when compared to a thermosetting composite tow). This makes steering quite difficult without the creation of various process induced defects, such as bridging and tow wrinkling. In addition, providing an adequate amount of heat necessary to efficiently bring the composite to its optimum processing temperature is quite a challenge in an AFP process as it limits the materials that can be used in the heated zone.

The past, current, and future research on the fabrication methods and associated equipment used for manufacturing VSC will first be presented. Due to a variety of manufacturing constraints, several types of defects are induced by the manufacturing process. A review of these defects, their effects on the laminates, and the inclusion of these defects into the design analysis will also be discussed. Finally, the research objectives and experimental procedures will be detailed. The experimental setup will be detailed, leading to a discussion of the experimental results and development of the AFP process.

CHAPTER 2 LITERATURE REVIEW

One of the first investigations of the use of continuous fibers whose directions vary across the domain was performed by Hyman et al in 1967 [6]. A specimen was fabricated by hand, using unidirectional fibers and inserting a cylindrical rod through a hole that was made by manually separating the fibers, all before adding the resin and initiating the curing process. These specimens were tested to failure under uniaxial tension then compared to a variety of different laminate designs. The authors identified a need for more advanced fabrication techniques, as several specimens with steered fibers showed very poor tensile strength.

Clearly, the fabrication of composite laminates with steered fibers is of great importance. Influenced by automated manufacturing techniques such as ATL and FW, the fabrication of VSC laminates is performed with a process called automated fiber steering (AFP). In order to optimize this manufacturing process and the VSC design, process parameters such as the minimum turn radius, tool path, and process variabilities must be analyzed and incorporated into the design space.

2.1 EARLY DEVELOPMENTS

In order to improve the quality and cost-effectiveness of manufacturing laminated composites, automation of the layup process has been adopted. For components used in the aerospace industries, where a high level of quality is required, the use of processes

such as ATL and FW helps reduce layup errors and material waste [7]. These processes led to the development and application of AFP, where narrow strips of fibers are collocated onto a tool in order to build up a composite laminate. This process was applied to the fabrication of VSC laminates, with one of the earliest tow placement systems used being the Viper Fiber Placement System from Cincinnati Machines. As early as 2002, Wu et al used this fiber placement system for the manufacturing of VSC laminates out of AS4/977-3 graphite-epoxy pre-preg material [8].

Automated tape layup is a form of additive manufacturing, where unidirectional pre-preg composite tape is placed onto a tool surface by a specialized automated machine. The use of this type of process includes high layup rates, capability to manufacture large parts, capability to handle high areal weight materials, and simplified offline machine programming. The disadvantages of such a system include high initial capital expenditure, and limited geometric complexity capabilities [8].

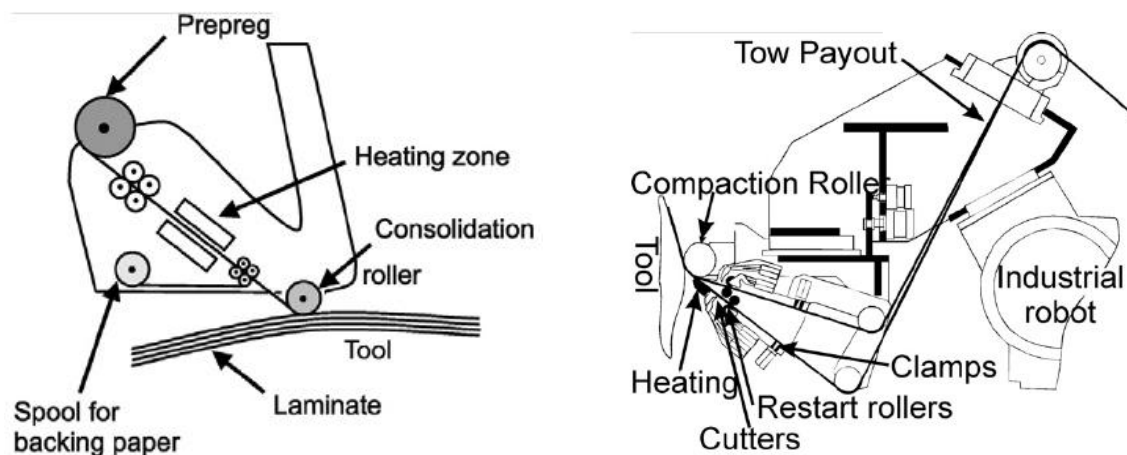


Figure 1.1 Schematic of an ATL head (left) [1] and an AFP head (right) [2]

Similar to ATL, AFP is a type of additive manufacturing with the significant difference being the material being laid down. Where ATL typically uses unidirectional tape of widths from 75 to 300 mm, AFP systems use unidirectional composite tows of widths from 3.2 to 12.7 mm. Due to the small tow width, AFP machines deliver multiple tows in parallel with each other simultaneously with some systems able to deliver up to 32 tows [7].

One of the earliest fiber placement machines was developed by Goldsworthy in 1974, where he tackled the challenge of consolidating unidirectional composite tape onto a curved surface [9]. The use of AFP systems for thermoplastic materials began in the late 1980s, with Grove authoring one of the earliest publications that details the development of a thermoplastic composite layup [2]. In 1995, Mondo investigated the resulting interlaminar shear strength of thermoplastic composite structures manufactured using AFP [1].

For more information on the historical developments regarding ATL and AFP, please refer to the literature review published by Lukaszewicz et al [7]. The authors go into great detail when reviewing both manufacturing systems, even detailing the application of AFP to the manufacturing of VSC laminates. As the benefit of designing VSC laminates involves orienting the fibers in the optimum direction, determining the limitations of the manufacturing process and incorporating these constraints into the design space is of critical importance.

2.2 MANUFACTURING CONSTRAINTS

Ideally, the design of VSC laminates will result in a laminated composite structure whose fiber orientations maximize the components physical properties for the

given structural requirements. Several constraints associated with the manufacturing of VSC laminates may cause the final laminate design to vary from the idealized solution, however.

2.2.1 FIBER PLACEMENT TURN RADIUS

One such constraint is the minimum turn radius of the fiber. The minimum curvature that the fiber path can follow depends on the material properties of the fiber, the width of the tow, and of the tooling involved. One of the first steps to developing realistic VSC laminate designs was taken by Gürdal and Olmedo, introducing a fiber path definition where the fiber angle orientations vary linearly across the laminate [10].

Parnas et al first incorporated a curvature constraint into their design methodology, where the radius of curvature for each point on the fiber path is constrained to prevent fiber breakage. Later, Setoodeh et al used an algorithm based on the cellular automata paradigm in order to address discontinuities in the fiber paths, constraining the fiber angle distribution across the domain using strains and material properties [11]. While the proposed methodology resolved some of the manufacturing issues associated with the design of a VSC laminate, they were unable to produce a design that can be realistically fabricated.

Van Campen et al continued this research, converting a LP distribution of a VSC laminate design into a realistic stacking sequence design in terms of fiber angles. In using the CA framework, the authors were able to include a manufacturing constraint on the in-plane curvature of the fibers [12]. In addition, this methodology allows for the inclusion of additional constraints on the fiber angle distribution, allowing for the design of a realistic VSC laminate whose fiber paths in each ply have been optimized.

2.2.2 PROCESS INDUCED DEFECTS

In 2002, Moon et al provided an evaluation of manufactured VSC laminates and reported that the number of defects developed in the manufacturing process is a function of the smallest steering radius [1]. When steering the tows, the outer fibers must travel a farther distance than the inner fibers. Since the fibers are inextensible, the combination of process parameters (compaction pressure, process temperature, etc.), turning radius, tow width, and matrix material properties may cause several defects such as tow buckling or pull up. In addition, the manufacturing of VSC laminates creates gaps and overlaps due to process variabilities and the width of the tows with respect to the fiber paths. Ideally, each tow would be placed in parallel with each other and have no overlaps or gaps as a result. In order to address this problem, AFP machines must cut and restart individual tows. This creates tow drop regions that may either cause gaps, overlaps, or a combination of the two defects.

Blom et al studied the effect of tow drop areas on the resulting strength and stiffness of the laminate with varying tow widths and number of plies. By staggering the location of the tow drop areas, the authors were able to minimize the overall thickness buildup in the laminate. In addition, it was found that increasing the tow width correlates to a reduction in strength, as the size of the tow drop areas (gaps) increases. The location of these tow drop areas also has an effect on the strength reduction, with the effects being mitigated by tow drop staggering [1]. This work was extended by Blom et al, developing a method for designing a VSC laminate for minimum thickness. It was shown that the amount of gap and overlap affects the structural response, manufacturing time, and surface quality of the finished product [13].

The location of these tow drop regions was the focus of the study by Fayazbakhsh et al, where a procedure was developed for identifying tow drop regions from a VSC structure design. In addition to identifying the location of gaps and overlaps, the area percentages of these defects was also calculated in relation to the tow widths and manufacturing parameters [14].

The effects of process induced defects on the mechanical properties of the ultimate tensile strength of a VSC laminate was investigated experimentally by Croft et al. Loading conditions and the part geometry change the effects of the defects, which add more complexity to the analysis. In order to simulate the effects of the defects created, theoretical configurations were used for: gaps, overlaps, half-gap/overlap, and twisted tow [15].

It was found that tolerance-induced defects happen repeatedly in all layers and they can be situated on top of each other, with the thickness variation being inversely proportional to the thickness of the laminate. In addition, it was shown that tows have the ability to move according to the previous layers and fill all possible gaps, regardless of size [15]. The authors also identified that fiber waviness needs to be taken into consideration when evaluating the effects of process induced defects on a laminate level. The majority of the fiber waviness resulted from the pressure pushing other plies onto the defects.

Fayazbakhsh later proposed a defect layer methodology to characterize the changes in mechanical properties of each layer in a VSC laminate as a result of process induced defects [16]. MATLAB subroutines were developed in order to identify the location and these defects and calculate the defect area, ultimately maximizing the in-

plane stiffness and buckling load simultaneously of a laminate with embedded defects. Two representative designs with an optimum fiber path were selected in order to investigate the effects of gaps or overlaps, using a constant curvature fiber path presented by Blom [11] for offsetting the subsequent fibers. Investigating a complete gap and complete overlap strategy for manufacturing the VSC laminate, the authors observed that the gaps deteriorate both in-plane stiffness and buckling load whereas overlaps improve the overall structural performance.

Nik et al continued the work from Fayazbakhsh [16] and obtained a Pareto front for the optimum design of VSC where buckling load and in-plane stiffness are simultaneously optimized with the inclusion of gaps and overlaps. The authors investigated how the parameters governing the formation of defects impact the set of optimal solutions for a multi-objective optimization problem, where in-plane stiffness and buckling load are simultaneously optimized. It was found that increasing the number of tows and decreasing the tow width results in the minimization of gap and overlap area percentages within the laminate [17].

2.3 TOOL PATH DESIGN

Just as the design space for VSC laminates increase to include manufacturing defects, the design of the respective tool path must also progress in order to increase the overall quality of the part. Understanding the limitation of the AFP tooling and its tool path allows the design methodology to be updated to result in a laminate design that can be manufactured and is fully optimized for a given set of conditions. In addition, minimizing the overall process time is of critical concern. Reducing the overall cost of

manufacturing VSC structures helps increase the feasibility of implementing these parts into various industries.

Shirinzadeh et al published an early study that described a process planning techniques and formulations for the application of AFP to achieve fiber steering [18]. Debout et al presented a method to improve the kinematic behavior of a 7-axis AFP machine by smoothing the tool path, reducing the manufacturing time while ensuring a requested level of quality [19]. The authors detailed two methods in order to achieve this objective:

1. Tool path smoothing achieved in the machine coordinate system using a filtering method which reduces the error of the roller orientation caused by deformation of the end effector during operation.
2. Determining an objective criterion to minimize manufacturing time for a given tool path, using the redundancy of the machine to optimize the control of joint coordinate values.

The application of both these methods, named *Piecewise filtering method*, reduced the manufacturing time by 32.9%. Testing revealed that smoothing of the tool axis orientation does not impact the quality of the part if the tool remains within a specific area, the domain of admissible orientation (DAO). Inside the DAO, which is determined by the manufacturing constraints, the tool orientation can be smoothed while respecting the required quality [19].

Bruyneel and Zein presented a new approach for defining fiber placement trajectories based on the Fast Marching Method, a numerical method used for the

simulation of moving interfaces. This algorithm for determining fiber trajectories over 3D surfaces was demonstrated to be effective at minimizing gaps and overlaps [20].

The problem of generating accurate tool paths for placing composite tows on a complex surface for the fabrication of a high quality laminate was also addressed by Yan et al. A roller path planning method was proposed that ensures a specified amount of gaps and overlaps. A set of surface curves is formulated to represent the tool path, taking into account the distance between the roller and the mold and the surface change as a result of completing a layer [21].

2.4 THERMOPLASTIC COMPOSITES

While a majority of the AFP, ATL, and FW manufacturing processes use pre-preg composites with thermosetting resins, there are several researchers and manufacturers that perform in-situ consolidation of thermoplastic composites. Tessnow published a review of the design, development, and testing of a thermoplastic composite support structure for the ducted tail rotor and vertical fin of a Bell helicopter [22]. This component was manufactured using an AFP machine from Automated Dynamics out of unidirectional carbon fiber with a PEEK matrix material (AS4/APC-2). Pasanen, Morris, and Hethcock utilized AFP processes to manufacture a horizontal stabilizer (spars, trailing edge, and ribs) from a similar material [23]. Langone, Pasanen, Mondo, and Martin published their research into the optimization of in-situ consolidation of AS4/PPS composite tape by fabricating and testing NOL ring specimens [24].

2.4.1 HEATING REQUIREMENTS

As previously mentioned in chapter 1, the use of thermoplastic composites over thermosetting composites provide several advantages that may be desired for a particular

structure or component. The in-situ consolidation of these composites does come with a unique set of challenges that must be addressed during the AFP process.

The amount of heat necessary to consolidate the material is quite high when compared to the AFP of thermosetting composites. While pre-preg composite tows with a thermosetting resin only need to be heated in order to resume the curing process and make the resin tacky, thermoplastics require enough heat to bring the material to its melting temperature. Semi-crystalline thermoplastics, such as PEEK and PPS, also experience crystallization during the heating and cooling cycles in AFP that add an additional material parameter that is dependent on the manufacturing process.

Automated Dynamics addressed the crystallization of APC-2 during their AFP process, stating that crystallinity of up to 34% is achievable in a laminate [25]. While increasing the crystallinity increases the melting temperature during the layup, increasing the amount of heat necessary for in-situ consolidation, it also improves the resistance to solvents and ability to resist creep. In Sonmez and Hahn's work on modeling the ATL of AS4/APC-2, the crystallinity through the thickness of the laminate was found and show to be between 20% – 30% [3].

Heated gas heaters are common heat sources used for in-situ consolidation of thermoplastic composites. This system uses an inert gas heated past the melting temperature (for semi-crystalline thermoplastics) or an optimum process temperature above the Vicat softening temperature (for fully amorphous thermoplastics). In order to validate their model, Sonmez and Hahn used an AFP machine equipped with a heated gas heater that was capable of heating their material to a temperature of 750°C [3]. Some of

Automated Dynamic's AFP machines also utilize a heated gas process that heats nitrogen to 975°C [25].

Laser heating is also used for various in-situ consolidation processes, such as ATL, AFP, and FW. Sonmez and Hahn compared laser heating to heated gas for their AFP analysis, showing the achievable roller speeds as a function of the roller radius for a given heat input [3]. Automated Dynamics also published a review of their work on implementing laser heating with their AFP machine, a heating solution that allows for greater control of the heat input due to its high energy density and rapid response [25][25][25], [26]. In their material selection and process analysis for thermoplastic fiber placement, Sharp, Holmes and Woodall also developed a laser heating system to be used with their Ingersoll fiber placement machine [5].

CHAPTER 3 RESEARCH OBJECTIVES

By developing a specialized process for using thermoplastic impregnated, unidirectional carbon-fiber along with AFP, it would be possible to gain the benefits of spatially varying the tows across the laminate while further reducing the associated manufacturing costs. In order to successfully automate the manufacturing of variable stiffness thermoplastic composites, the new process will have to be very specialized. The equipment used in the manufacturing process will have to be developed from the ground up to not only manufacture the composites but precisely measure and control all of the process parameters in-situ. This research aims to develop an AFP process that can be extended to research the fabrication of VSC thermoplastic laminates. By developing the equipment and process needed, the viability of using AFS with thermoplastic composite tows will be determined.

To achieve this task, a 6-axis robot arm was used for automated fiber-steering while a stationary experimental fiber placement head was developed for dispensing the individual tows. Upon developing this experimental setup, the influence of the various process parameters on the quality of a resulting constant stiffness laminate was investigated. The tows used for fiber placement consisted of thermoplastic impregnated carbon-fiber. Two different systems of heating were compared and the effect of using

secondary rollers with a primary compaction roller on the in-situ consolidation process was investigated.

Lastly, the experimental results from this research will be applied to the future development of a truly automated system that can be used for manufacturing VSC laminates. In order to complete the development of an AFS process, additional technical challenges will have to be investigated and addressed. These challenges will be discussed and potential solutions will be proposed for inspiring future research in the manufacturing of variable stiffness thermoplastic composites.

3.1 MATERIAL SELECTION

The materials used in this AFP process are carbon-fiber tows with a PEI thermoplastic matrix. This allows for the minimization of noise factors while still developing the AFP process for a high performance thermoplastic that can be used in a wide variety of components and industries. The tow width was kept constant at 1/8" width and only a single tow will be placed at a time. This further reduced the number of variables and possible noise. While the small tow width results in longer process times, it allows for a smaller turning radius when fiber steering.

The material being used is sourced from TenCate Advanced Composites. It is a carbon/PEI tape, slit to 1/8" tows by Web Industries, and consists of Hexcel HexTow® AS4 unidirectional carbon fiber with Sabc ULTEM™ PEI resin as the matrix. Provided by TenCate, the mechanical properties for the slit tape is listed in table 3.1.

Table 3.1 Typical Mechanical Properties for Cetex TC1000 (PEI), AS4, 145gsm, 32% RC

Property	Testing Standard	Average Result	
0° Tensile	ASTM D 3039	Strength, MPa	2241
		Modulus, GPa	127.6
0° Compression	ASTM D 3410	Strength, MPa	930.8
		Modulus, GPa	120.7
0° Flex	ASTM D 790	Strength, MPa	1655
		Modulus, GPa	124.1
90° Tensile	ASTM D 3039	Strength, MPa	65.50
		Modulus, GPa	8.963
90° Flex	ASTM D 790	Strength, MPa	999.7

Due to the number of missing material properties for the slit tape being used, the material properties for both the PEI resin and the carbon fiber are listed below in tables 3.2 and 3.3, respectively.

Table 3.2 Typical Material Properties for ULTEM™ Resin 1000

Mechanical Properties	Testing Standard	Average Result	
Tensile Stress, Yield, Type 1, 5 mm/min	ASTM D 638	1120	kgf/cm ²
Tensile Strain, Yield, Type 1, 5 mm/min	ASTM D 638	7	%
Tensile Strain, Break, Type 1, 5 mm/min	ASTM D 638	60	%
Tensile Modulus, 5 mm/min	ASTM D 638	36500	kgf/cm ²
Flexural Stress, Yield, 2.6 mm/min, 100 mm span	ASTM D 790	1680	kgf/cm ²
Flexural Modulus, 2.6 mm/min, 100 mm span	ASTM D 790	35800	kgf/cm ²
Physical Properties	Testing Standard	Average Result	
Specific Gravity	ASTM D 792	1.27	-

Water Absorption, 24 hours	ASTM D 570	0.25	%
Water Absorption, equilibrium, 23°C	ASTM D 570	1.25	%
Melt Flow Rate, 337°C/6.6 kgf	ASTM D 1238	9	g/10 min
Thermal Properties	Testing Standard	Average Result	
Vicat Softening Temp, Rate K/h	ASTM D 1525	218	°C
HDT, 0.45 MPa, 6.4 mm, unannealed	ASTM D 648	210	°C
HDT, 1.82 MPa, 6.4 mm, unannealed	ASTM D 648	201	°C
CTE, -20°C to 150°C, flow	ASTM E 831	5.58E-05	1/°C
CTE, -20°C to 150°C, xflow	ASTM E 831	5.4E-05	1/°C
Thermal Conductivity	ASTM C 177	0.22	W/m-°C

Table 3.3 Typical Material Properties for HexTow® AS4 6K Carbon Fiber

Mechanical Properties	Testing Standard	Average Result	
Tensile Strength	-	640	MPa
Tensile Modulus	-	33.5	GPa
Ultimate Elongation at Failure	-	1.7	%
Physical Properties	Testing Standard	Average Result	
Density	-	1.79	g/cm ³
Weight/Length	-	0.427	g/m
Tow Cross-Sectional Area	-	0.240	mm ²
Filament Diameter	-	7.1	Microns
Carbon Content	-	94.0	%
Thermal Properties	Testing Standard	Average Result	
Specific Heat	-	0.27	cal/g-°C
Coefficient of Thermal Expansion	-	-0.63	ppm/°C
Thermal Conductivity	-	6.83	W/m-°K

3.2 AUTOMATED FIBER PLACEMENT

In order to fabricate a VSC laminate out of thermoplastic composites, an automated manufacturing process needs to be developed where the tows can be compacted and steered in-situ. Currently, very few companies and research groups are able to utilize an AFP process for the fabrication of constant stiffness thermoplastic laminates. In order to achieve this goal, a scaled down experimental fiber placement machine was developed where a single tow can be placed at a time.

This experimental setup allows for the characterization of a manufacturing process for automated fiber placement. Each process parameter can be controlled and monitored during the layup, allowing for research to be performed on the fiber placement of thermoplastic fiber placement. This research can then be extended to the manufacturing of a VSC component. It is important that this process, and the experimental AFP machine, can be used to steer fibers and not just place tows for a constant stiffness design.

3.2.1 MACHINE DEVELOPMENT

The experimental setup that was developed consists of a stationary fiber placement head and a heated tool mounted on an articulated robotic arm. The fiber placement head allows for various heat sources to be mounted and tested, as well as for a variety of rollers to be used. This setup is designed to be very configurable, allowing a variety of experiments to be performed on the same machine. The heated tool allows for the substrate temperature to be controlled while the articulated robot arm that it is mounted on allows for control of the feed rate, fiber direction, and layup orientation. In

addition, creating a scaled down AFP machine with a very configurable form-factor allows for the process to be characterized with minimal initial costs.

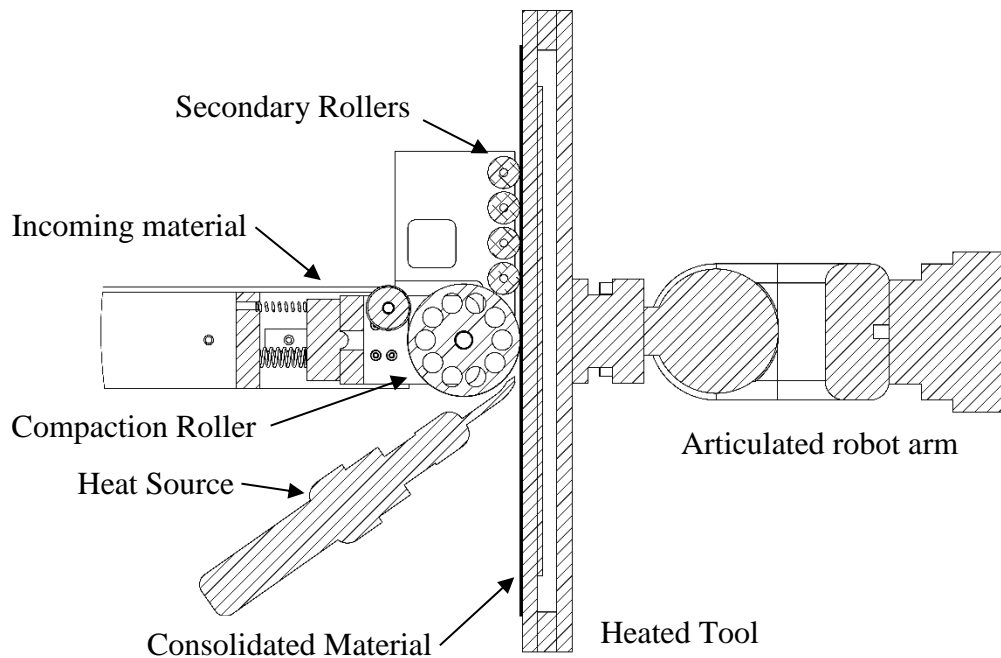


Figure 3.1 Experimental AFP Machine

The design requirements for the experimental AFP machine consist of the following:

- Ability to control and monitor the relevant process parameters
- Test and use multiple heat sources
- Heat the tow being consolidated well past its glass transition temperature, reaching a maximum of 500 °C
- Provide in-situ consolidation of the Carbon/PEI tow
- Be modular to allow for process improvements and modifications

Along with these requirements, the design of this experimental setup was developed by identifying the process variables that affect the layup during automated fiber placement. Table 3.4 displays the relevant signal, control, and noise variables for the AFP process. The signal variables constitute the independent variables that can be altered to affect the output of the process. The various parameters that have an effect of the output but are not controllable throughout the process are listed as control variables. The process variability is caused by variability in the machine operation, material quality, environment, and human interaction. These are noise variable, which can be minimized to improve the process efficiency and layup quality but not eliminated.

In order to identify the optimum set of process parameters that result in a layup of excellent quality, every effort was made in the design and fabrication of the experimental AFP machine to minimize noise, maximize control, and monitor the signal variables.

Table 3.4 Process Variables

	Man	Machine	Materials	Environment
Signal Variables	Tool Design Laminate Design	Compaction Force Feed Rate Tow Path Tow Tension Primary Heat Application Tool Temperature Secondary Heat Application		
Control Variables	Tool Preparation	Substrate Cooling Heat Source Start and Stop Position Roller	Substrate Material Tow Dimensions Tow Material	
Noise Variables	Material Handling	Positional Variability Tool Compliance AFP Head Compliance	Tow Defects Tow Properties Moisture Content	Temperature Moisture

By determining the optimum process window, identifying the key process parameters, and necessary future research that must be performed, a more advanced AFP machine can be developed in order to increase process throughput and expand the research on VSC manufacturing.

3.2.2 PROCESS CHARACTERIZATION

In order to investigate the influence of each process parameter and develop an optimum process window, several experiments were performed where relevant control factors were varied. This allows for specific interactions to be investigated while minimizing noise and redundant trials. These experiments are described in table 3.5 and will be referenced again in section 4.1 when discussing the design of experiments.

Table 3.5 Experiment Descriptions

Experiment	Description	Control Factors	Label
1	Vary the heat application at various distances to the substrate for different heat sources	Heat source Distance to substrate Primary heater temperature Tool Temperature	H h T_h T_t
2	Vary primary heater, secondary heater, and tool temperatures to maximize feed rate	Feed rate Primary heater temperature Secondary heater temperature Tool temperature	f T_h T_{AFP} T_t
3	Vary tow tension and compaction force to maximize feed rate	Feed rate Tow tension Compaction force	f F_t F_c
4	Vary the number of rollers and tow tension to maximize feed rate	Total number of rollers Feed rate Tow Tension	N_r f F_t
5	Vary the feed rate according to the number of plies	Feed Rate Ply number	f n

The heating temperature indicates the temperature setting of the primary heat sourced used to bring the material up to an optimum consolidation temperature. It is very difficult to acquire an accurate temperature achieved by the material itself; therefore, thermocouples are used with the primary heat source in order to achieve a level of control on the amount of heat being applied.

The tool being used for consolidation is heated to a constant temperature T_t . In addition, the AFP head is also heated to a temperature T_{AFP} in order to create a heated zone that allows for control over the temperature gradient from the tool to the AFP head during consolidation. This minimizes the effect that the environmental temperature has while increasing control on the overall heat application. Additional signal variables that will be monitored and controlled include the compaction force, tow tension, and feed rate.

The motivation behind the 5 experiments comes from the ability to most easily control the primary heater, compaction force, and feed rate. Overall, the success of each experiment will be judged by the quality of the laminate and the process throughput. As a result, it is critical that the effect each process parameters has on the feed rate be investigated closely.

In addition, there are also several control variables that have been investigated to see their effect on the process. The use of additional rollers and tool preparation has on the overall efficiency and layup quality was investigated. Lastly, how the feed rate changes as the number of plies increase is investigated.

3.3 PROCESS EVALUATION

In order to quantify the success of the various experiments and thoroughly characterize the process, the resulting layup and AFP process must both be evaluated to a set standard. Rather than provide a qualitative analysis of the process, however, this research aims to provide a quantitative process analysis that may assist in determining any potential industrial applications and identifying what areas of the manufacturing process must be improved.

The layup is compared to a similar laminate produced with a hot press. A laminate fabricated with a hot press provides a control sample of superior quality, as the time, temperature, and pressure can be precisely controlled in a manner not achievable in an AFP process. Tensile testing fabricated composite specimens provide a qualitative assessment of the bond strength, while surface quality and tow position variability are analyzed to further qualify the AFP process. Any process induced defects, such as wrinkling, bridging, or tow twist will be identified. The positional variability of the fiber placement will also be analyzed by measuring tow straightness and parallelism. Failure of the AFP process will be determined by a weak bond, were the tow being placed is easily removable from the substrate. The tow should be bonded across the entire area with little to no gaps with the substrate caused by wrinkling and bridging of the tow or previously compacted material. Lastly, the ability to fabricate a $[0, 45, 90, -45]_s$ laminate will be used as a final proof of concept for the resultant manufacturing process.

CHAPTER 4 EXPERIMENTAL PROCEDURES

4.1 DESIGN OF EXPERIMENTS

In order to determine the influence each process parameter has on the quality of the laminate and the overall process speed, a set of experiments was developed by following the Taguchi methodology. This design of experiments (DOE) is a statistical technique for determining the optimum set of process parameters in order to improve process performance, minimize noise, and decrease the number of experimental trials necessary to achieve statistically relevant results.

The experiments performed aim to maximize the material feed rate, bond strength, and quality of the laminate. Mixes of two- and three-level partial factorial experiments were performed. Initially, these experiments were qualified by whether consolidation of the material was achieved and if no delamination was caused by the process. This approach was adopted in order to understand the relationship between the control factors and narrow to process window. In addition, the success of the in-situ consolidation is judged via single lap shear tests. Failure of the test specimen as a result of fiber fracture or in-plane shear failure of the joint at a stress near the shear strength of the matrix material is considered a success in the consolidation of the material. Once this was accomplished, more focused experiments were performed where the tow straightness/parallelism is improved and waviness is minimized. These future

experiments should be coupled with a true sensitivity analysis in order to fully characterize the process and allow for research into modeling the process to begin.

The results of these experiments are compared to the findings of various publications on the in-situ consolidation of thermoplastic composites. Nejhad published an investigation on the issues related to the in-situ consolidation of APC-2 composite (PEEK thermoplastic matrix material) for tape laying and filament winding [27]. Sharp et al also published an investigation on the issues related to in-situ consolidation of APC-2 composites, where AFP was employed to manufacture a cylindrical component [5]. Sonmez and Hahn later published their analysis of an in-situ consolidation process for automated tape layup of same material [3]. The findings of their research analyze the effects of many of the same process parameters this paper is investigating and provides a good reference for analyzing the experimental results.

4.1.1 HEAT SOURCE INVESTIGATION

Before experimental trials on consolidating the tows in-situ can begin, an investigation was performed on two different heat sources. The viability of hot air or infrared heaters as a suitable heat source for the AFP of carbon/PEI tows was evaluated.

The heat source being employed needs to bring the material being consolidated to a minimum temperature of 317 °C and heat a concentrated area in order to avoid deforming or delaminating the surrounding material that has already been placed. There are bounds on the amount of heat that can be applied, as thermal degradation can occur if the PEI is held at elevated temperatures for too long. Both Carroccio et al [28] and Li [29] report that PEI undergoes thermal degradation starting at around 400 °C. These two

heat sources were chosen because they allow for heating of the material well past its glass transition temperature, can provide concentrated heating, and are very cost effective.

The heaters are tested at various distances from the heated tool, where a thermocouple is used to measure the temperature increase of the material being heated after a given amount of time. The distance to the material, temperature setting of the heater, and tool temperature setting are control factors while the temperature increase in the material is measured and recorded for each experiment. Table 4.1 below shows the control factors and their settings.

Table 4.1 Control Factors for Experiment 1

Control Factor	Label	1	2	3
Heater	A	<i>H1</i> <i>Hot Air</i>	<i>H2</i> <i>IR</i>	
Distance to the surface	B	<i>h1</i> 10	<i>h2</i> 15	
Heater Setting (°C)	C	<i>T_{h1}</i> 450	<i>T_{h2}</i> 400	<i>T_{h3}</i> 350
Tool Temperature Setting (°C)	D	<i>T_{t1}</i> 140	<i>T_{t2}</i> 120	<i>T_{t3}</i> 100

The distance to the surface was tested for two additional settings ($h = 20$ mm, 25 mm); however, the results were universally poor as neither heat source could reasonably heat. Due to the mixed number of levels when testing each of the control factors listed above, it was most beneficial to perform a full factorial experimental design where every combination of factor settings is tested.

The result of these experimentations show the discrepancy of the heater setting to the temperature of the material (for the hot air heater), the influence of distance of the heater to the steady state temperature reached by the material, and the maximum temperature increase achievable by each heater. Table 4.2 shown below details the experimental design in detail.

Table 4.2 Full Factorial Design for Experiment 1

Trial Number	Control Factors			
	<i>A</i>	<i>B</i>	<i>C</i>	<i>D</i>
1.	1	1	1	1
2.	1	1	2	1
3.	1	1	3	1
4.	1	1	1	2
5.	1	1	2	2
6.	1	1	3	2
7.	1	1	1	3
8.	1	1	2	3
9.	1	1	3	3
10.	1	2	1	1
11.	1	2	2	1
12.	1	2	3	1
13.	1	2	1	2
14.	1	2	2	2
15.	1	2	3	2
16.	1	2	1	3
17.	1	2	2	3
18.	1	2	3	3
19.	2	1	1	1
20.	2	1	2	1
21.	2	1	3	1
22.	2	1	1	2
23.	2	1	2	2
24.	2	1	3	2
25.	2	1	1	3
26.	2	1	2	3
27.	2	1	3	3
28.	2	2	1	1
29.	2	2	2	1
30.	2	2	3	1
31.	2	2	1	2
32.	2	2	2	2
33.	2	2	3	2
34.	2	2	1	3

35.	2	2	2	3
36.	2	2	3	3

4.1.2 FEED RATE AND HEAT APPLICATION CORRELATION

The second experiments performed investigate the correlation of heater temperature settings and tool temperature to the feed rate. From preliminary trials that were performed, as well as experiment 1, it was determined that following process parameters with the hot air heater (table 4.3) provided acceptable consolidation of the material:

Table 4.3 Baseline Process Parameters for Experiment 2

f (mm/s)	T_h (°C)	T_{AFP} (°C)	T_t (°C)	F_c (N)	F_t (N)	n	M_r	N_r
0.5	480	480	150	314	5	2	304 Stainless Steel	4

For this experiment, the roller material was stainless steel while the total number of rollers used remained 4. In addition, the compaction force was held at 314 N and a minimum tow tension of 5 N was used. Lastly, the number of plies been compacted on was kept at 2. The list of control factors being varied is shown below in table 4.4, where their settings are listed explicitly for each of the 3 levels.

Table 4.4 Control Factors for Experiment 2

Control Factor	Label	1	2	3
Feed rate (<i>mm/s</i>)	A	<i>f1</i> 0.3	<i>f2</i> 0.4	<i>f3</i> 0.5
Primary heater temperature (°C)	B	<i>T_{h1}</i> 480	<i>T_{h2}</i> 460	<i>T_{h3}</i> 440
Secondary heater temperature (°C)	C	<i>T_{AFP1}</i> 480	<i>T_{AFP2}</i> 460	<i>T_{AFP3}</i> 440
Tool temperature (°C)	D	<i>T_{t1}</i> 150	<i>T_{t2}</i> 140	<i>T_{t3}</i> 130

The runs performed were organized using a 3-element orthogonal array of four levels. Unlike the full factorial design for experiment 1, each trial for experiment 2 was performed 3 times, resulting in a total of 27 runs. The experimental design is shown below in table 4.5.

Table 4.5 Orthogonal Array $L_9(3^4)$ for Experiment 2

Trial Number	Control Factors			
	A	B	C	D
1.	1	1	1	1
2.	1	2	2	2
3.	1	3	3	3
4.	2	1	2	3
5.	2	2	3	1
6.	2	3	1	2
7.	3	1	3	2
8.	3	2	1	3
9.	3	3	2	1

4.1.3 COMPACTION FORCE AND TOW TENSION INVESTIGATION

The second experiment investigates the impact that tow tension and compaction pressure have on the consolidation of the material. Like the last experiment, the number of plies and rollers, as well as the roller material was held constant. In addition, the number of plies being consolidated on remained 2. The feed rate, compaction force, and tow tension was varied between 3 different levels while the primary heater, secondary heater, and tool were set to 480 °C, 480 °C, and 150 °C respectively.

This experiment aims to identify the affect that compaction force and tow tension have on the process. This is especially important because with the roller size and roller are set, therefore the only way that compaction pressure can be controlled is by altering the compaction force. In addition, the high temperatures needed bring the material to its optimum processing temperature eliminate many roller materials that may allow for a large contact width. As a result, being able to control the contact force throughout the manufacturing process is critical. Table 4.6 below list the control factors and their settings at 3 different levels.

Table 4.6 Control Factors for Experiment 3

Control Factor	Label	1	2	3
Feed rate (<i>mm/s</i>)	A	f_1 0.3	f_2 0.4	f_3 0.5
Compaction force (<i>N</i>)	B	F_c1 314	F_c2 220	F_c3 157
Tow tension (<i>N</i>)	C	F_t1 5	F_t2 10	F_t3 15

These control factors were tested using a 9-run, 3-element orthogonal array of 3 levels. The 9 trials were performed 3 times, resulting in a total of 27 runs. The experimental design is shown below in table 4.7.

Table 4.7 Orthogonal Array $L_9(3^3)$ for Experiment 3

Trial Number	Control Factors		
	<i>A</i>	<i>B</i>	<i>C</i>
1.	1	1	1
2.	1	2	2
3.	1	3	3
4.	2	1	2
5.	2	2	3
6.	2	3	1
7.	3	1	3
8.	3	2	1
9.	3	3	2

4.1.4 ADDITIONAL ROLLER INVESTIGATION

The manufacture specifications for the composite tows being tested recommend an initial cure temperature of 317 °C. At these temperatures, the possible materials that can be used to fabricate an acceptable roller are quite narrow when compared to consolidating thermo-setting composite tows. The roller material must be able to maintain its surface quality at those elevated temperatures throughout the entire layup, as well as withstand the pressures during compaction.

Stainless steel is an excellent material to fabricate a compaction roller out of; however, the material stiffness creates a very small contact width when compared to some of the polymer rollers used for the layup of thermos-setting composite tows. Even at very large diameters, this causes the dwell time to be extremely small when only using

1 roller. By increasing the number of rollers, however, it may be possible to increase the dwell time and improve the in-situ consolidation by introducing more tension in the tows being compacted.

Increasing the total number of rollers reduces the overall pressure on the material and alters the amount of tow tension that should be used. While a sufficient amount of pressure must be applied to the material, too much has detrimental effects and may cause delamination [3]. Due to this, it is very interesting to investigate the interaction between the total number of rollers, compaction force, and tow tension for maximizing feed rate. Table 4.8 below lists the control factors and their settings for 3 different levels. Similar to experiment 3, both the primary and secondary heaters were set to 480 °C and the tool temperature was set to 150 °C.

Table 4.8 Control Factors for Experiment 4

Control Factors	Label	1	2	3
Total number of rollers	A	N_r1 2	N_r2 3	N_r3 4
Feed rate (mm/s)	B	$f1$ 0.3	$f2$ 0.4	$f3$ 0.5
Compaction force (N)	C	F_c1 314	F_c2 220	F_c3 157
Tow tension (N)	D	F_t1 5	F_t2 10	F_t3 15

As experiment 4 consists of 4 control factors being varied at 3 different settings, resulting in the same degrees of freedom as experiment 2, the same orthogonal array is used for this experiment. Table 4.5 can be used to reference the design of this experiment.

4.1.5 FEED RATE AND PLY NUMBER INVESTIGATION

After investigating the effects compaction force has on the process, it is a natural progression to look into how the process varies after multiple plies have been laid. In order to do this, 2 separate full factorial designs were used where the feed rate and compaction force was varied. The settings for these control factors are listed below in tables 4.9, 4.10, and 4.11 for a total number of plies being laid-up on of $n = 3$, $n = 5$ and $n = 7$, respectively.

Table 4.9 Control Factors for Experiment 5a ($n = 3$)

Control Factors	Label	1	2	3
Feed rate (mm/s)	A	$f1$ 1.0	$f2$ 2.5	$f3$ 2.0
Compaction force (N)	B	F_c1 314	F_c2 220	F_c3 157

Table 4.10 Control Factors for Experiment 5b ($n = 5$)

Control Factors	Label	1	2	3
Feed rate (mm/s)	A	$f1$ 2.5	$f2$ 2.5	$f3$ 3.0
Compaction force (N)	B	F_c1 314	F_c2 220	F_c3 157

Table 4.11 Control Factors for Experiment 5c ($n = 7$)

Control Factors	Label	1	2	3
Feed rate (mm/s)	A	$f1$ 3.0	$f2$ 3.5	$f3$ 4.0
Compaction force (N)	B	F_c1 314	F_c2 220	F_c3 157

These control factors are tested using a full-factorial experimental design. Due to the small number of controls factors and reasonable number of levels, it is possible to perform a run for every combination of control factors and settings. The experiment design is shown in table 4.12. These trials were performed for each of the experiments, resulting in a total of 27 runs.

Table 4.12 Full Factorial Design for Experiment 5

Trial Number	Control Factors	
	A	B
1.	1	1
2.	1	2
3.	1	3
4.	2	1
5.	2	2
6.	2	3
7.	3	1
8.	3	2
9.	3	3

There is an assumption being made that the feed rate will increase with the number of plies. This result has been reported by Sonmez and Hahn [3]. It was found that the maximum feed rate increased with the number of layers, due to the majority of the

consolidation occurring during placement of the subsequent layer. The exception to this was the last layer, where slow speeds were needed. The results of experiments 5a, 5b, and 5c will be compared with the trends shown in figure 4.1.

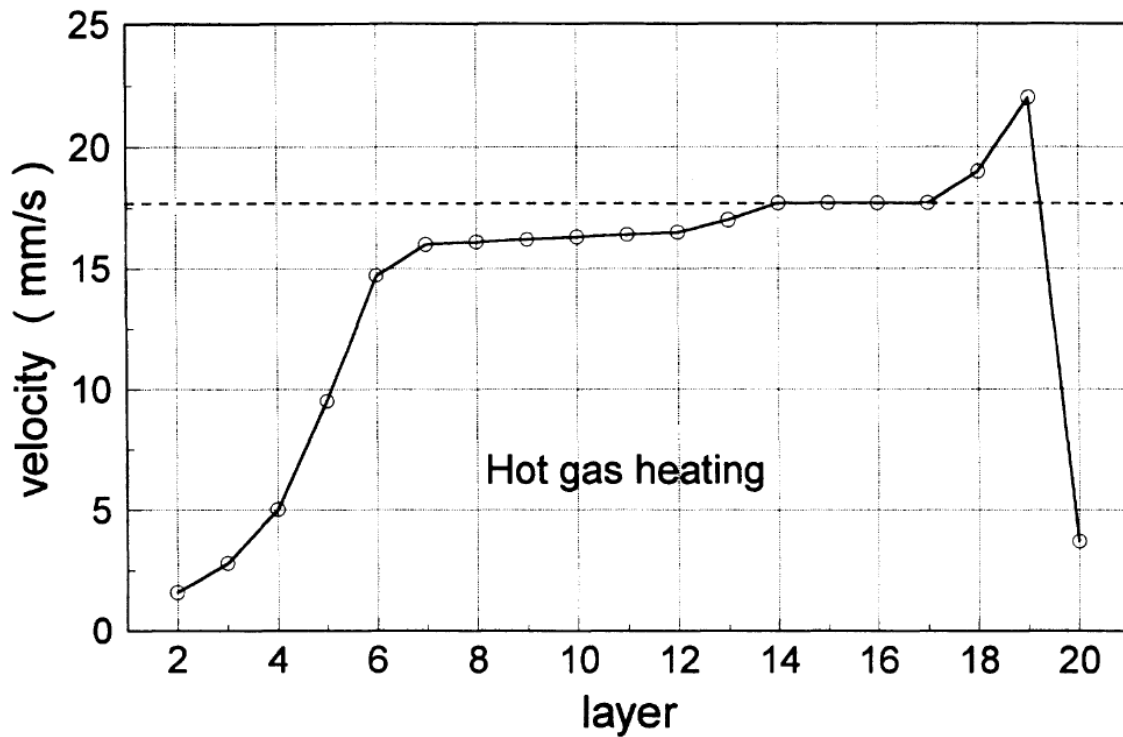


Figure 4.1 Feasible roller speeds for each layer during a 20-ply lay-up process with a preheat temperature of 150 °C [3].

4.2 TENSILE TESTING

The 2nd layer in-situ consolidation process is tested against a control by employing the ASTM D1002 single lap shear test. This test method allows for an analysis of the bond strength, where shear failure at the interface of the 2 plies indicate insufficient consolidation. The material is aligned along the fiber direction and

consolidated to create a [0/0] test specimen. The results of these tests influence the design of experiments 2 through 5 by correlating pressure application, feed rate, and heat flow to the consolidation of the 1st and 2nd layer of the composite.

4.2.1 TEST SPECIFICATIONS

The test specimens are manufactured to conform to the dimensions shown in Figure 4.2. The tow thickness is 0.2 mm, overall width is 12.7 mm, and overall length is 203.2 mm. The specimens made are tested in tension along the fiber direction at a loading rate of 0.05 in/min (1.27 mm/min).

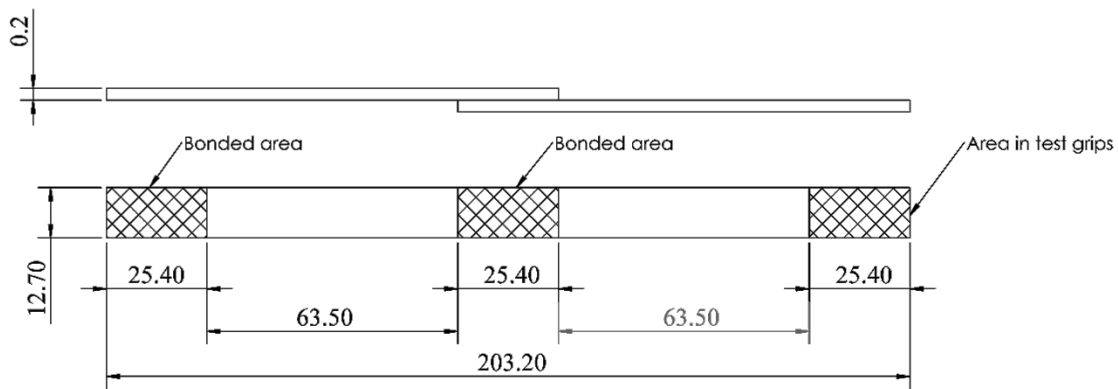


Figure 4.2 Single Lap Shear Specimen with [0/0] orientation

Both the bonded area and the area being held in the test grips are 25.4 mm long. This bonded area represent the area that each tow is in contact with each other during the consolidation process. The maximum bond length was found using the following equation [30]:

$$L = \frac{Fty * t}{\tau} \quad \text{Equation 1}$$

Where:

$L = \text{length of overlap (m)}$, $t = \text{thickness of tow (m)}$, $F_{ty} = \text{yield stress of the tow (Pa)}$, $\tau = 150\% \text{ of the average shear strength (Pa)}$

The average shear strength at the bonded area was assumed to be equal to that of ULTEM™ PEI, which has a shear strength of $\tau = 103.42 \text{ MPa}$. The maximum permissible length was found to be 28.9 mm. As a result, 25.4 mm (1 in) was chosen as the appropriate amount of overlap. This equation is usually applied in order to ensure that the yield stress of the specimen being tested is not exceeded and that the strength of the bond is actually tested. For these experiments, however, failure due to fiber fracture will still be considered as acceptable results. Failure of the in-situ consolidation process will be determined from in-plane shear failure of the bond area at a stress lower than the shear strength of the PEI thermoplastic resin.

4.2.2 CONTROL SPECIMENS

The control specimens are made using a hot plate where the pressure and temperature are precisely controlled to make a [0/0] laminate with only a 25.4 mm bonded area. Multiple specimens were cut from this specimen then tested using the same single lap shear specifications discussed in the previous section. Figure 4.3 below shows the laminate made with the hot press.

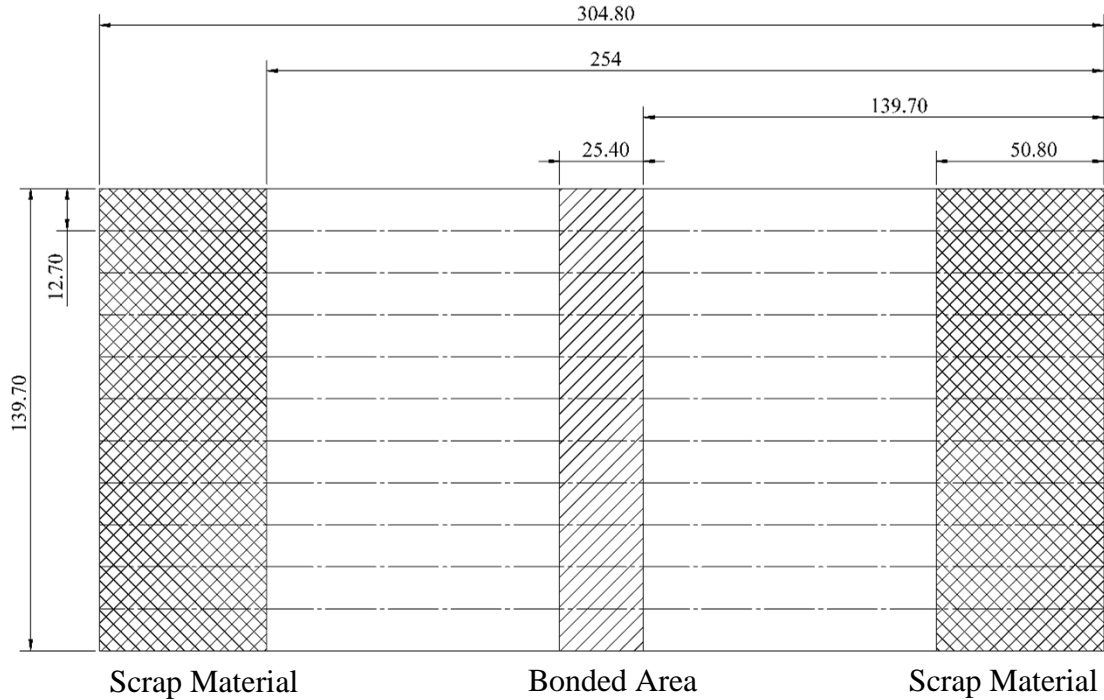


Figure 4.3 Control Specimens

The laminate was fabricated by heating it to 600 °F (315 °C) at a force of 0.3 ton (2.998 kN). The material was held at that temperature for 3 minutes then cooled at a rate of 20 °F a minute.

4.3 DRYING OF CARBON/PEI TOWS

All of the material used in this automated fiber placement process was dried prior to use. The amount of water that is absorbed by the PEI matrix material may cause quite a bit of problems during consolidation. Research performed by Li [29] report that PEI begins undergoing thermal degradation at around 460 °C due to scission of the imide group of the polymer chain from trace water being present. As a result, it is very important to dry the material to ensure that the thermoplastic is thermally stable.

The drying process was performed according to the specifications recommended by SABIC. The composite tape was dried at a temperature of 140 °C for 6 hours. In addition, excess material was taken out of the experimental setup and dried again every 2 weeks to ensure that a moisture content of 0.02% is never exceeded.

CHAPTER 5 PRELIMINARY EXPERIMENTAL SETUP

5.1 OVERVIEW

In order to accomplish the experiments described in chapter 4, an experimental AFP machine needed to be developed where the relevant process parameters can be monitored and controlled while minimizing noise. This experimental setup differs from commercial AFP machines by being scaled down and highly modular. The benefits of this setup include a minimization of complexity, where tow cutting, automated start and stop capabilities, and multi-tow placement is eliminated. While this greatly reduces the overall throughput, it does allow for the investigation of the interaction of various process parameters with the minimum amount of noise. Other benefits include the ability to modify the experimental setup to accommodate new knowledge and additional processes with minimum downtime and expenses.

The experimental setup includes a stationary fiber placement head, a heated tool mounted on an articulated robot arm, a removable spool with a drag braking system for unidirectional tow feeding, and Ethernet connectivity for process monitoring and control. The design of this experimental setup followed the flow chart shown in figure 5.1.

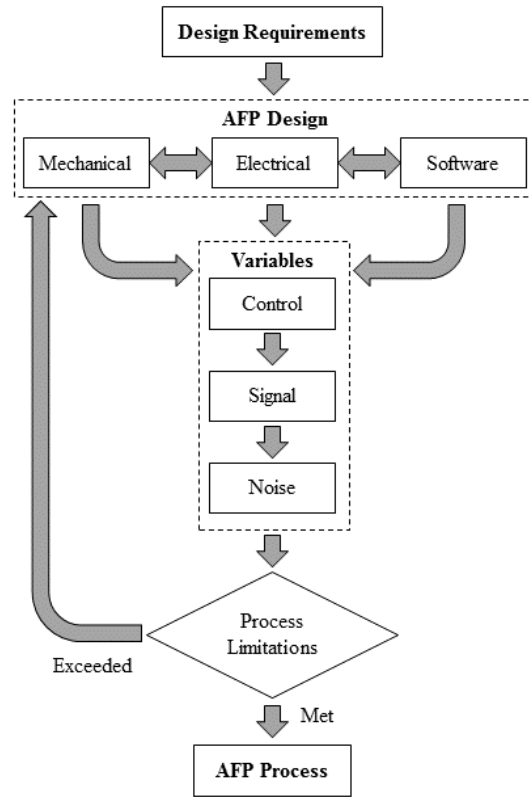


Figure 5.1 AFP Design Flow Chart

The design requirements influence the mechanical, electrical, and software design of the experimental AFP machine. These designs are all interdependent and influence the process variables that will be controlled and monitored. The signal variables must be able to be controlled in-situ while relevant data such as compaction force, tool temperature, and heating temperature are recorded.

While this experimental setup is not fully automated, this research will influence the design of a second iteration of an AFP machine for thermoplastic fiber steering. The next experimental setup should include feedback control, automated start and stop, and

multi-tow feeding capabilities in order to improve the process throughput. This will allow for research to be performed for production scale components.

5.2 FIBER PLACEMENT HEAD

The AFP head consists of a compaction roller, secondary rollers, a primary heat source, and a secondary heat source. This head allows for the TC1000 tow to be consolidated under pressure and tension. In addition, this fiber placement head allows for the addition secondary rollers. Figure 5.2 shows the AFP head with a 4 roller setup and with 2 hot air heaters.



Figure 5.2 AFP Head with 4 Roller Setup

The compaction roller is made of 304 stainless steel, allowing for a polished roller surface that resists wear and does not adhere to the tow being placed. The secondary rollers are made of 7075-T6 aluminum, as the primary purpose is to introduce additional tension into the tow being placed rather than compacting the material under heat. This allows for a less than perfect surface quality. The dimensions and position of these rollers are shown in figure 5.3.

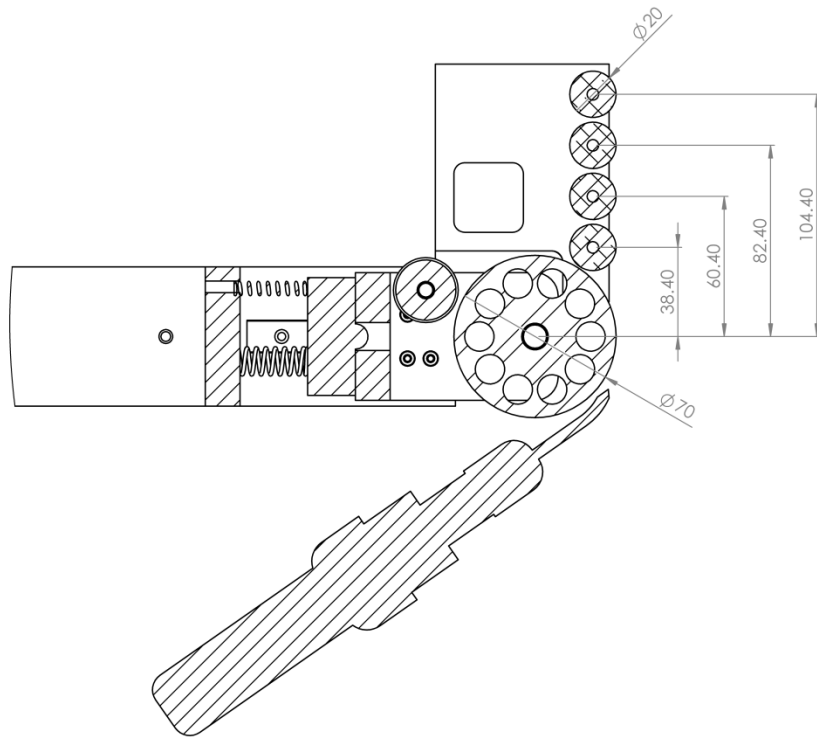


Figure 5.3 AFP Head Cross-Section with Dimensions

The rollers and heat sources are spring mounted on linear guides to allow for control of the compaction force while accommodating for dimensional variance in the tool surface and position. In addition, a compression load cell is fitted in line with the

rollers and the springs in order to provide constant monitoring of the compaction force. Figure 5.4 below displays the compaction force as a function of compaction roller displacement. The position of the heated tool, and subsequently the displacement of the compaction roller, is controlled by positioning the articulated robot arm.

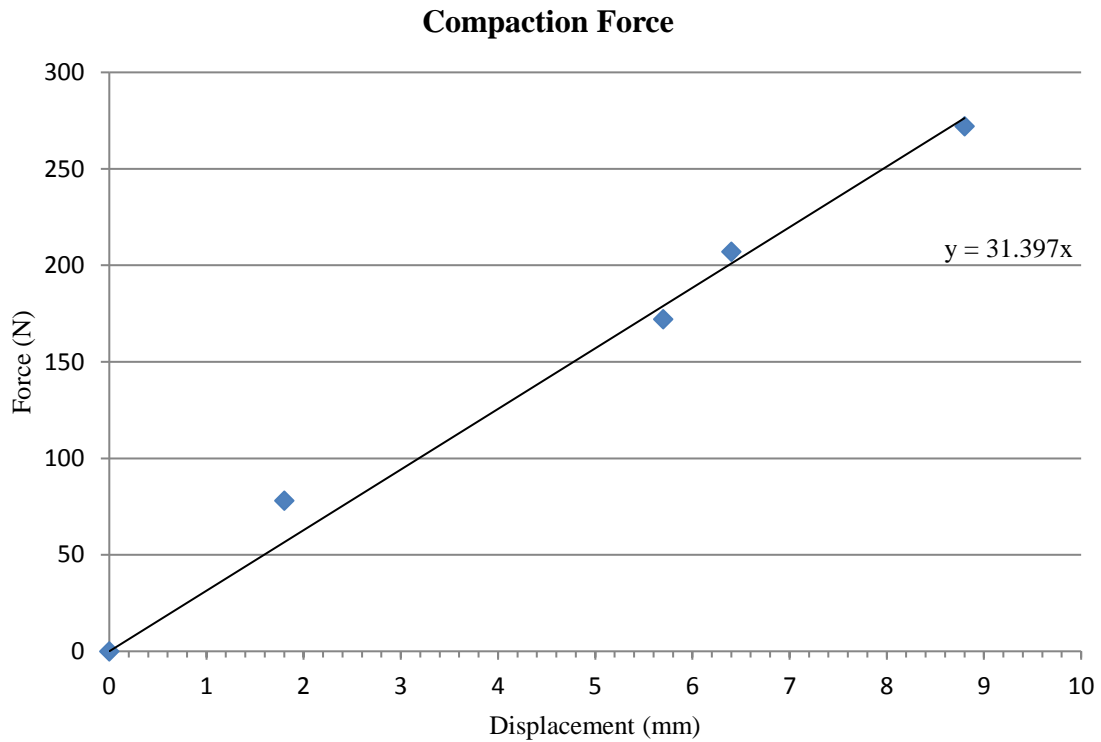


Figure 5.4 Compaction Force vs. Roller Displacement

5.3 HEAT SOURCES

Two different heat methods are being tested: hot air and infrared. Heated gas and infrared heating are two widely used methods for the heating of thermoplastics in FW and ATL. The two heaters chosen allowed for the concepts to be tested against each other in a

cost effective manner. These heaters needed to be able to heat a concentrated area of the material to a minimum of 317 °C.

The hot air heater consists of a modified HA welder typically used for soldering electronics. This system allowed for heating of air to a temperature of 480 °C with additional control of the flow rate. This heater was modified with a heater tip that allows for a more concentrated heating of the tow being placed, as well as being wired into the electrical system to allow for automated control during fiber placement. Figure 5.5 shows the heater being used and the modified tip.



Figure 5.5 303D Hot Air Rework Station and Modified Heater Tip

The infrared heater being tested consists of a handheld infrared welder modified with a double convex lens. The lens is a 35 mm diameter lens with a 70 mm focal length. This setup allows for a relatively low cost, 600W IR heater to be used for concentrated

heating of the material (not the surrounding air) up to 480 °C very quickly. Figure 5.6 shows the IR heater being tested, with the only modification being the lens.



Figure 5.6 T835 Solder Station

5.4 FIBER TENSIONER

The TC1000 tow being placed is kept in tension using a spool with a friction based drag brake system. This spool is removable and allows for simple changing of the material if needed. In addition, the mounting of this spool allows for quick repositioning, allowing for multiple rows of material to be wound on the same spool and used without needing to remove the spool. Figure 5.7 shows this system in detail.



Figure 5.7 Repositionable Spool with Drag Braking System

In addition to the drag braking system, a spring based tensioner is placed in-line with the tow before the AFP head. This mechanical tensioner allows for measuring of the tow tension with either a caliper (using the known spring constant) or a digital force gage. These two systems together, allow for unidirectional tensioning of the tow that can be adjusted for various trials. Figure 5.8 below shows this mechanical tensioner fitted with a force gage.

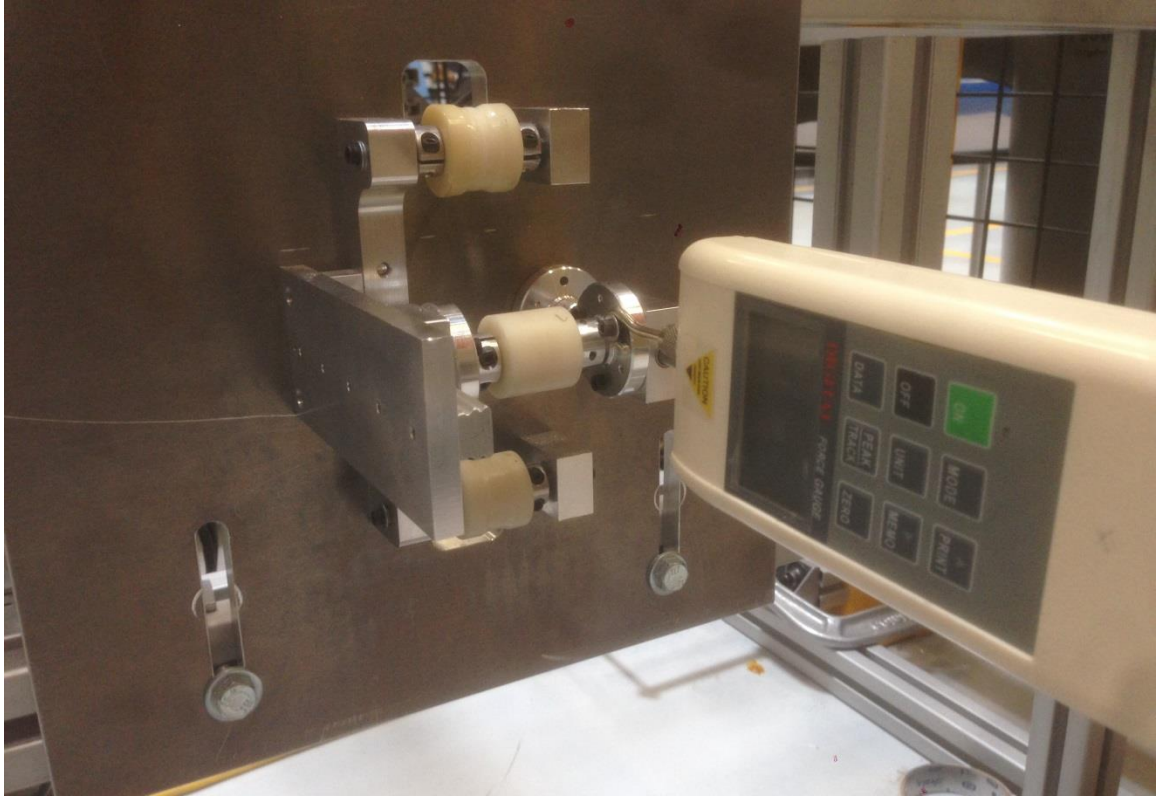


Figure 5.8 Mechanical Tensioner with Fitted Force Gage

5.5 HEATED TOOL

The tool on which the laminate is being consolidated on is a machined flat plate mounted onto an articulated robot arm. In order to heat the substrate and material that has been consolidated, the mounted tool is heated using a flexible silicon heating pad. This allows for the surface of the tool to reach a steady state temperature of 150 °C. This heating pad is connected to a PID controller that allows for the tool temperature to be maintained within ± 3 °C. This setup can be seen in figure 5.9 below.

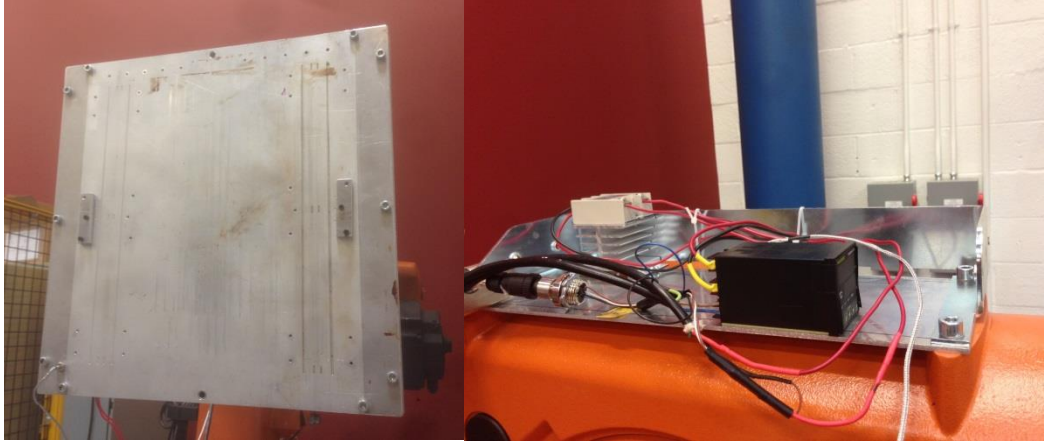


Figure 5.9 Heated Tool and PID Controller Setup

Sonmez and Hahn [3] reported a direct increase in compaction roller speeds with the pre-heating temperature. While it is possible to cause delamination by heating the material too much, it is generally desirable to preheat the tool to the highest possible temperature.

5.6 INTEGRATION WITH ARTICULATED ROBOT ARM

With the AFP head being fixed in place, the tool is moved relative to the head via 6-DOF articulated robot arm. The heated tool is mounted on a KUKA KR60 which is programmed to move the tool through the appropriate tool path. By programming the position, velocity, and tool path of the KR60, the feed rate and compaction force throughout the tow path can be controlled.

Control of the heat sources and data collection is possible by communicating with the KR60 via an EtherCAT fieldbus system. A digital output terminal allows for any of the heat sources to be turned on/off by the KR60 controller, while a thermocouple terminal allows for data to be collected from up to 8 thermocouples. In addition, an

analog input terminal allows for infrared temperature sensors (such as the OMEGA[®] OS136 Sensor) or compression load cells (OMEGA[®] LC305) to be connected to the system. Figure 5.10 shows this EtherCAT fieldbus system as it is connected on the experimental setup.

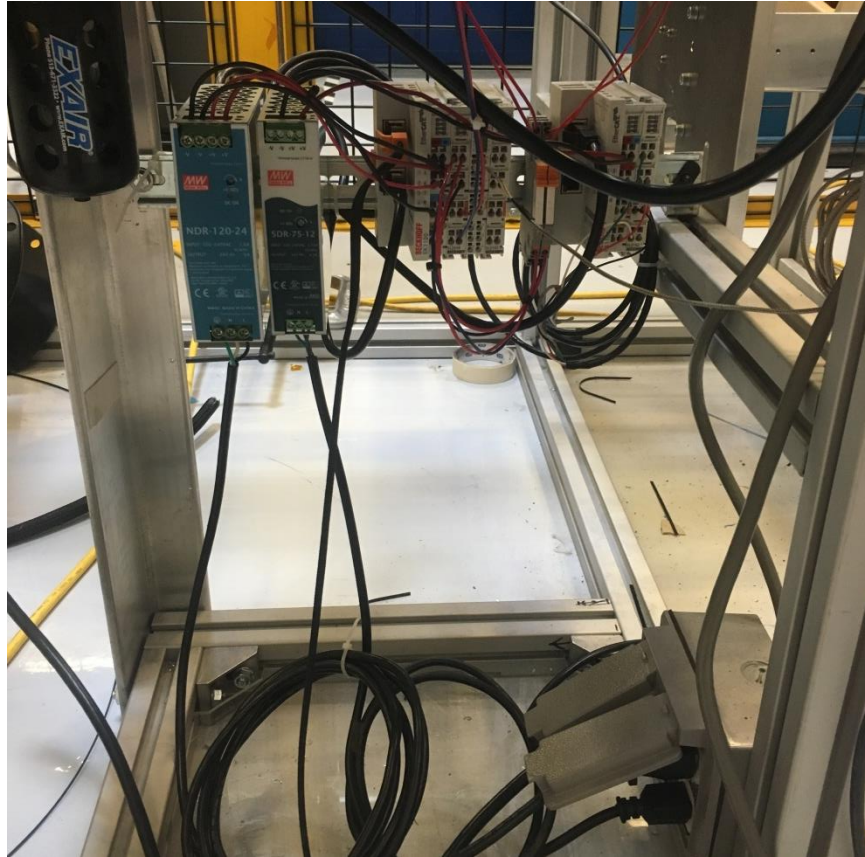


Figure 5.10 EtherCAT Fieldbus System and Power Supply

The heat sources are turned on/off throughout the AFP process, however, control of the temperature must be set beforehand. The sensor readings are recorded throughout the entire process and can be stored and written to a text file allowing for post-process

analysis. Lastly, additional sensors and equipment can be added to this system, such as solenoids for pneumatic actuation or stepper motors for automated tow feeding.

CHAPTER 6 RESULTS AND ANALYSIS

6.1 HEAT SOURCE COMPARISON

Before completing the development of the AFP experimental setup, two different off-the-shelf welders were tested and compared: a hot air welder and a handheld infrared welder. The ability of each heater to bring the tow to its recommended processing temperature (317 °C) and size of their effective heating areas were analyzed.

6.1.1 HOT AIR HEATER

With a 1/8" inner diameter tip fitted, the hot air welder worked very well for heating a single tow with minimal heating of the surrounding area. When analyzing the effect of tool temperature on the resulting temperature of the material being heated, there was a dramatic effect when increasing the tool from 100 °C to 120 °C. The difference in the average temperature of the material when increasing from 120 °C to 140 °C, however, is negligible. This can be seen in figure 6.1, where the average temperatures reached by the material are plotted against the heater temperature setting.

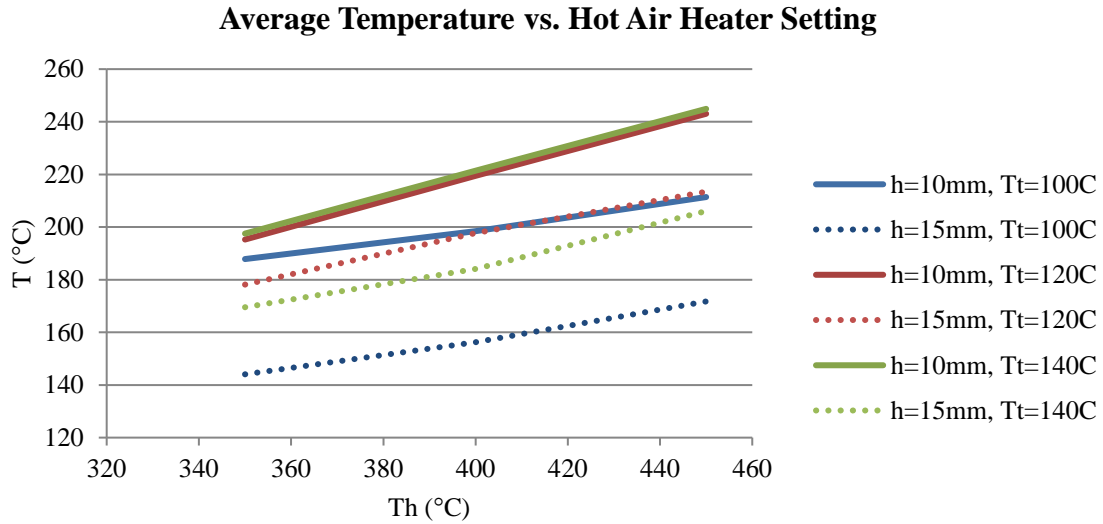


Figure 6.1 Average Material Temperatures vs. HA Heater Temperature Setting

Figure 6.1 also shows the dramatic affect that the distance of the heater tip to the material plays on the resulting material temperature. Table 6.1 below displays the average and maximum temperatures reached by the material at both distances tested, where $T_h = 450\text{ }^\circ\text{C}$ and $T_t = 140\text{ }^\circ\text{C}$. In addition, the length of time until the material reached a steady state temperature is also listed.

Table 6.1 Material Temperatures Reached for $h_1 = 10\text{ mm}$ and $h_2 = 15\text{ mm}$

Distance to Tool Surface, h	mm	10	15
Average Temperature, T_{avg}	$^\circ\text{C}$	244.9	206
Max Temperature, T_{max}	$^\circ\text{C}$	247	210
Time to Steady State, t_{ss}	s	60	50

When analyzing how the heater setting affects the resulting material temperature, it was seen that the distance h affects the difference in temperature reached by the material. A 50 °C change in the heater temperature setting results in roughly a 23.5 °C change in the material temperature when $h = 10 \text{ mm}$. This difference markedly decreases when the distance increases to $h = 15 \text{ mm}$. Most importantly, there was a dramatic difference in the hot air heater temperature setting to the temperature of the material and failed to bring the tow to its T_g of 317 °C for these settings. These results can be seen in figure 6.2, where material temperatures reached are plotted for various primary heater settings as a function of time.

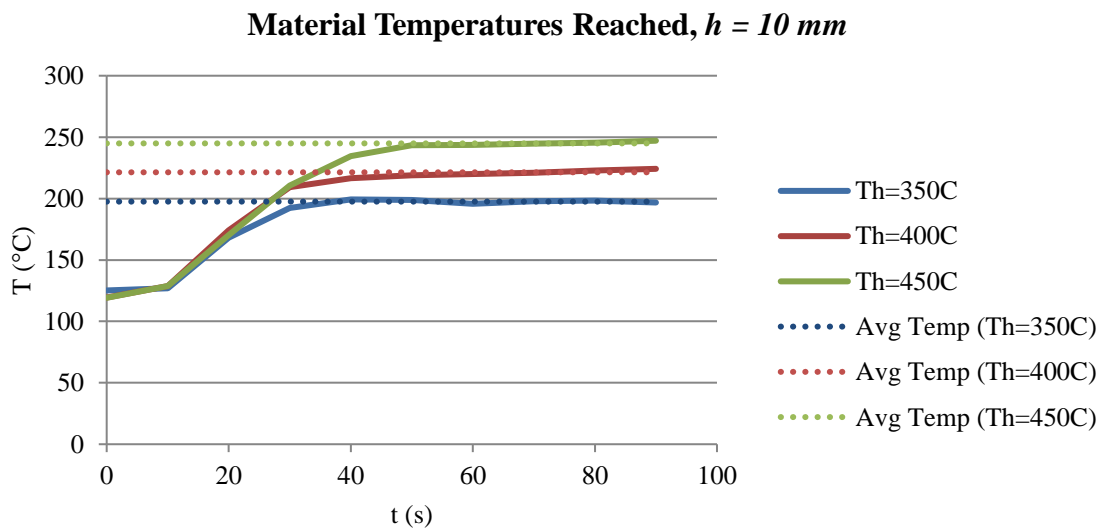


Figure 6.2 Material temperature as a function of time for $h = 10 \text{ mm}$

Decreasing the heater tip position to the material solved this problem, however. By bringing the heater tip to roughly 5 mm from the surface of the material, temperatures up to 420 °C were achievable at a tool temperature of $T_t = 150$ °C. With these adjustments, the hot air heating setup allowed for the correct amount of heating of the tow being placed and little of the surrounding material. This system does not leave much room for adjustment of the temperature; however, building on this concept and using a purpose built hot gas system will solve this. In addition, switching from air to an inert gas as the working fluid for heating is another modification that will allow for greater heating with less thermal degradation. For those reasons, this type of heating system is widely used in ATL [3] [2] and AFP [22] [31].

6.1.2 INFRARED HEATER

With the same experiments performed using the IR heater (experiment 1, trials 19 – 36), it became immediately clear that the most important parameter influencing the material temperature reached is distance to the tool. At the distances tested, the IR heater with the double convex lens failed to bring the material up to the pre-set heater temperature. By bringing the heater to a distance of roughly 5 mm, however, the material heated up extremely quickly. This can be seen in figure 6.3, where the temperature reached by the material is plotted against time for a distance of $h = 5$ mm and a tool temperature of $T_t = 150$ °C.

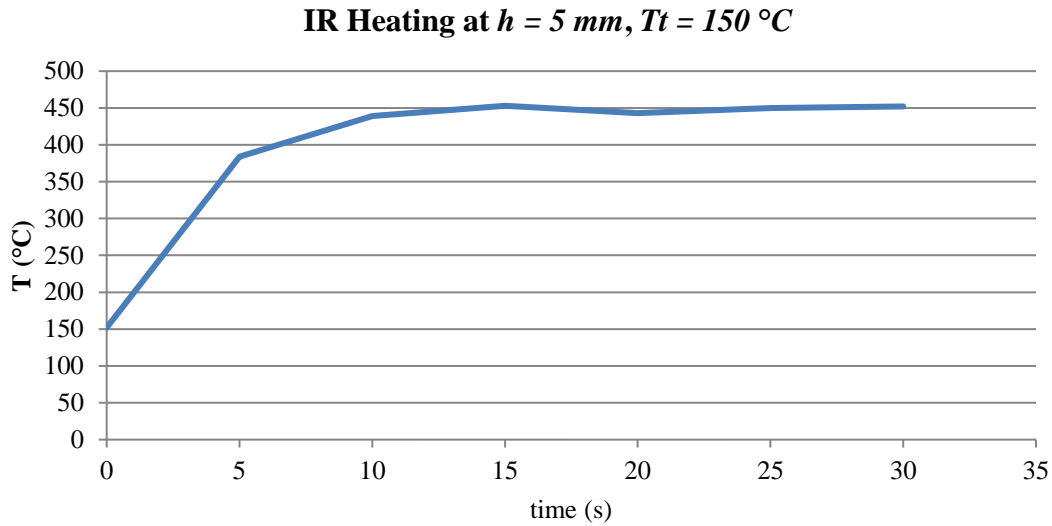


Figure 6.3 IR heating over time with $h = 5 \text{ mm}$, $T_t = 150 \text{ }^\circ\text{C}$

The time taken to reach a steady state temperature reached is very quick, reaching the set temperature of $450 \text{ }^\circ\text{C}$ in roughly 5 seconds. Once it reaches the appropriate temperature, the programming set by this heater cuts power and causes the temperature to drop roughly 8 degrees before it begins heating it back to the pre-set temperature. This is a problem that can be corrected with a purpose built IR heater with variable light intensity.

While the ability to heat the material to very high temperatures extremely quickly makes this system much more powerful than the HA system that was tested, the heated area was far too concentrated to be used effectively. In addition, this system requires that the heater is very close to the material and is exactly perpendicular to the tool surface. This means that the heater must be between two compaction rollers or compliant shoes. While these problems made this heating system a bit too unwieldy for the rest of the

experiments, designing a new AFP head and IR heating system made to work synergistically may yield great benefits. Higher material throughput may be achieved at a fraction of the cost of a laser heating system with a higher amount of control than a hot gas system.

6.2 HEATING LIMITATIONS

6.2.1 PRIMARY HEAT APPLICATION

The results of experiment 2 showed a clear result when it came to identifying the affect heating the material being fed has on the maximum feed rate that is achievable. With a HA system, the maximum temperature that the system can reach (480 °C) is the minimum temperature that was feasible for this experimental setup. The feed rates necessary for consolidation of the material is still too low to warrant reducing the primary heater temperature. While the feed rates do improve significantly at higher number of layers, there is still little reason to lower the heater temperature as no noticeable degradation was observed. The relationship between the number of layers and the feed rate will be discussed in a later section.

There are some constraints that must be taken into account, however. While increasing the applied should directly improve the feed rate, thermal degradation of the thermoplastic may occur as a result. Li [29] reported significant thermal degradation of PEI near 535 °C. It is important to note that this was found using a heating rate of 10 °C/min, resulting in a total time of 13.5 minutes where the material was between 400 °C to 535 °C. During the AFP process, this overall soak time is significantly less and may allow for elevated temperatures to be used in the process. This concept was discussed by

August et al in their publication detailing the AFP process developed by Automated Dynamics® [25].

6.2.2 SECONDARY HEAT APPLICATION

By using a stainless steel compaction roller, a significant amount of the heat applied to the tow being placed is absorbed and dissipated by the roller. In addition, using a larger diameter roller to increase the feed rate would magnify this problem. In order to combat this problem, it was necessary to use a secondary HA heater that allowed for heating of the compaction roller and heat affected zone. The placement of the secondary heater, along with the heat shield setup, can be seen in figure 6.4.

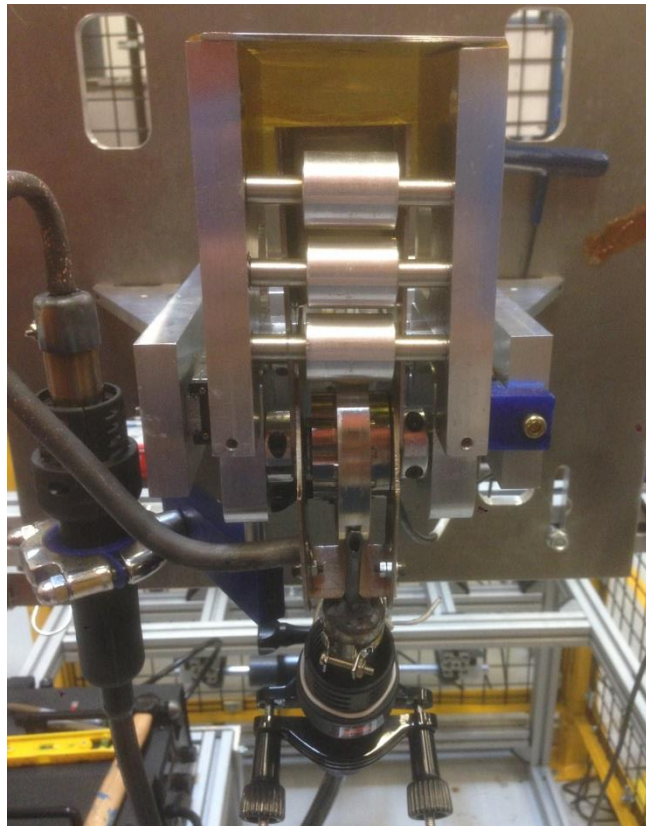


Figure 6.4 Secondary and Primary Heater Positioning

This secondary heated was able to increase the temperature of the main and secondary rollers to roughly 150 °C by setting the temperature to a maximum setting of 480 °C. Improving the heat shielding and better managing the heat flow will greatly decrease the heat losses. By increasing the overall temperature of the heat affected zone, more of the applied heat from the primary heater is absorbed by the material and promote polymer diffusion. In addition, the temperature gradient from the tool to the secondary rollers is minimized, allowing for a reduced cooling rate while the material is being compacted. Decreasing this temperature gradient is critical for eliminating delamination due to rapid cooling under a sudden release of compaction pressure and tension.

6.2.3 TOOL TEMPERATURE

As mentioned in section 6.1.1, heating the tool allows for increasing the maximum temperature reached by the material being placed. As a result, the overall feed rate is improved by increasing the tool temperature. The same result was reported by Sonmez and Hahn [3], where linear increases in roller speeds were achieved with increasing pre-heating temperatures. For the laminate layup, the tool temperature was kept at 150 °C. This was limited by the silicon heating pad, which became unreliable beyond 155 °C. With this combination of tool temperature, primary, and secondary heater settings, a temperature of roughly 500 °C was achieved at the nip region.

6.3 COMPACTION PRESSURE

6.3.1 INFLUENCE OF COMPACTION FORCE

Upon performing experiments 3 and 4, no correlation could be found between the compaction forces, number of rollers, and tow tension with feed rate. Altering the compaction pressure does indeed affect the degree of bond. The compaction pressure is a

function of compaction force, roller diameter, and number of rollers. Table 6.2 shows the maximum pressure at each of rollers for the 3 different compaction forces tested.

Table 6.2 Compaction pressure at each of the rollers (MPa)

Number of Rollers, N_r	4		3		2		
	Roller	Primary	Secondary	Primary	Secondary	Primary	Secondary
Compaction Force (N)							
$F = 314$		52.321	106.819	61.907	126.390	79.922	163.169
$F = 220$		43.795	89.412	51.819	105.793	66.898	136.579
$F = 157$		36.997	75.532	43.775	89.371	56.514	115.378

These pressures were found by measuring the compaction force and using the calculation for maximum pressure shown in Equation 2 below:

$$P_{max} = \frac{2F_c}{\pi bl} \quad \text{Equation 2}$$

This equation is used for calculation of Hertzian contact stresses, where b is the half width of the theoretical contact width of the roller to the material. It was found that if the compaction pressure was too low, consolidation did not occur regardless of the feed rate or the applied heat. In addition, increasing the compaction pressure too much negatively affect the bond as well. While 314 N was found to be the ideal compaction pressure based on the control factor settings chosen, no detrimental effects were seen from a range of 300 N to 320 N. Limitation in the experimental setup did not allow for increasing the load beyond 320 N.

As the numbers of rollers are decreased, the compaction force must also be decreased in order to consolidate the material being placed. Table 6.3 plots the decrease

in compaction force with the decrease in rollers for $T_h = 480\text{ }^\circ\text{C}$, $T_{AFP} = 480\text{ }^\circ\text{C}$, $T_l = 150\text{ }^\circ\text{C}$, and $f = 0.5\text{ mm/s}$.

Table 6.3 Optimum Compaction Force vs. Number of Rollers

Number of rollers, n	4	3	2
Compaction Force, F_c	314 N	226 N	163 N
Compaction Pressure	52.3 MPa	52.5 MPa	57.6 MPa

In order to better understand the mechanism causing the poor consolidation at elevated compaction pressures, Hertzian Contact Theory was used to determine the effective contact width, normal stress, and shear stress distribution for each of the rollers. Assuming an elliptical pressure distribution, the contact width can be found using the equation:

$$2b = K_b \sqrt{F_c} \quad \text{Equation 3}$$

Where:

$$K_b = \sqrt{\frac{2}{\pi l} \frac{(1 - \nu_1^2)/E_1 + (1 - \nu_2^2)/E_2}{1/d_1 + 1/d_2}} \quad \text{Equation 4}$$

The variables ν_1 and E_1 represent the Poisson's ratio and elastic modulus for the roller while l and d_1 represent the width and diameter. This analysis is assuming the tool is flat, therefore the d_2 is assumed to be infinite. The variables ν_2 and E_2 represent the Poisson's ratio and elastic modulus for the TC1000 tow being compacted upon.

The normal stress at the surface of the tow, where the roller and the material come into contact, is found using the following equation for the maximum pressure at the central line of contact:

$$\sigma_z = -P_{max} = -\frac{2F_c}{\pi bl} \quad \text{Equation 5}$$

Hertzian Contact Theory assumes an elliptical pressure distribution caused by the roller pressing on the surface of the tool. With the maximum normal stress and contact width known for the roller being using in this experimental setup, this assumption allows us to plot the pressure distribution. Figure 6.5 displays the pressure distribution for the primary roller at various compaction forces for a setup with 3 secondary rollers. Figure 6.6 displays the same analysis for the secondary rollers.

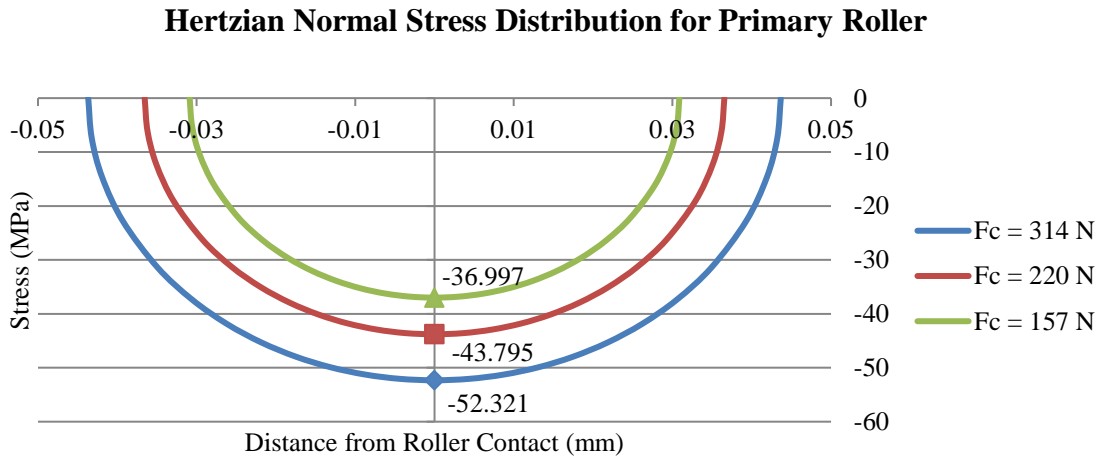


Figure 6.5 Normal Stress for Primary Roller vs. Compaction Force ($N_r = 4$)

Hertzian Normal Stress Distribution for Secondary Rollers

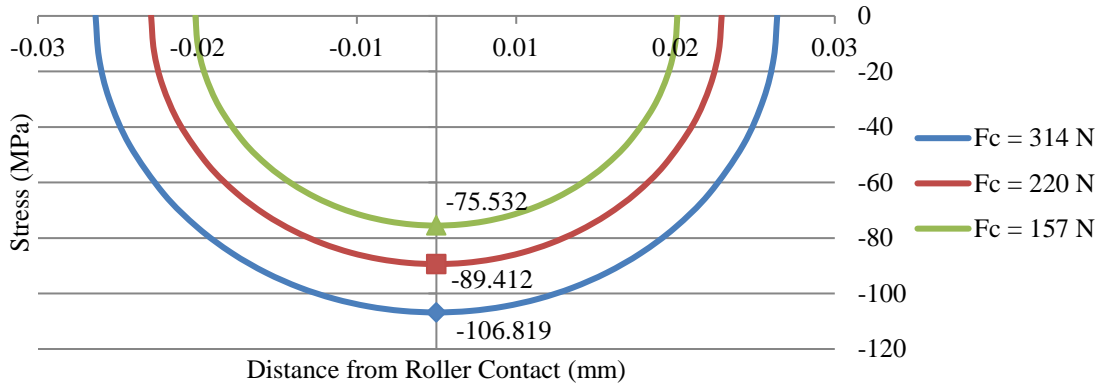


Figure 6.6 Normal Stress for Secondary Rollers vs. Compaction Force ($N_r = 4$)

While increasing the compaction force increases the contact width, allowing for a longer dwell time where the composite will be heated and under pressure, it also increases an already high normal stress. For a 4 roller setup, a compaction force of 314 N was found to result in acceptable consolidation of the material. This high pressure helps promote autohesion and reduce the formation of voids, however, the small contact width results in a very high stress concentration that should be avoided. This is caused by the relatively small roller size and the high stiffness of stainless steel.

In addition to looking at the normal stress at the surface of the tow, the shear stress through the depth of the material was also analyzed using the following expression:

$$\tau_{max} = \begin{cases} \tau_{13} = (\sigma_z - \sigma_x)/2 & \text{for } 0 \leq \zeta_b \leq 0.436 \\ \tau_{13} = (\sigma_z - \sigma_y)/2 & \text{for } 0.436 \leq \zeta_b \end{cases} \quad \text{Equation 6}$$

Where:

$$\zeta_b = \frac{z}{b} \quad \text{Equation 7}$$

And:

$Z = \text{distance below the material's surface}$

The maximum shear stress through the thickness of the material was plotted against for the three different compaction forces. This analysis is shown in figure 6.7 for a roller setup of $N_r = 4$.

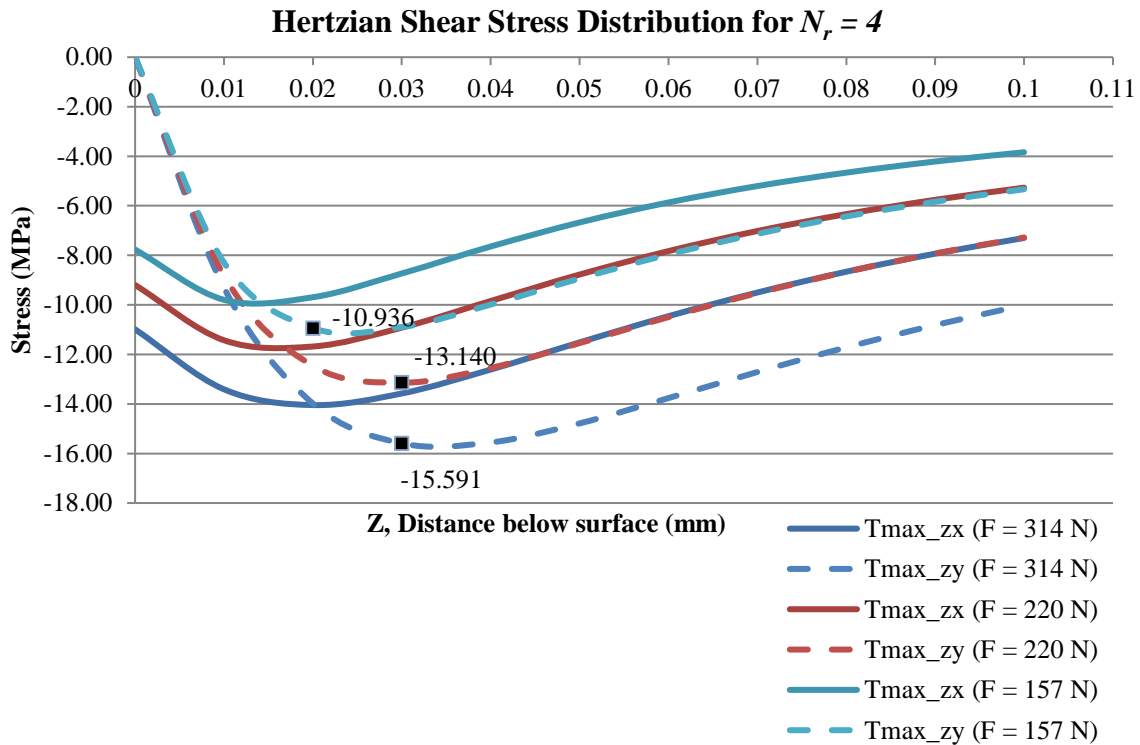


Figure 6.7 Shear Stress Distributions for Various Compaction Forces

While the shear stresses do increase for compaction forces as high as 314 N, this occurs at a depth between 0.3 mm and 0.4 mm and is relatively low when compared to the very high normal stress distribution. It must be noted that this analysis is performed with no heating of the roller or material being compacted. At the elevated temperatures

needed to consolidate the tow, these high stress concentrations pose a problem that must be managed with careful control of the compaction force.

6.3.2 ROLLER DIAMETER

While this experimental setup used a single compaction roller with a diameter of 70 mm, it appears that increasing the roller size will allow for higher feed rates. In order to analyze the effect of increasing the roller diameter, the contact width and normal stress was plotted against the roller diameter. This is shown in figure 6.8 for a stainless steel roller where $N_r = 4$.

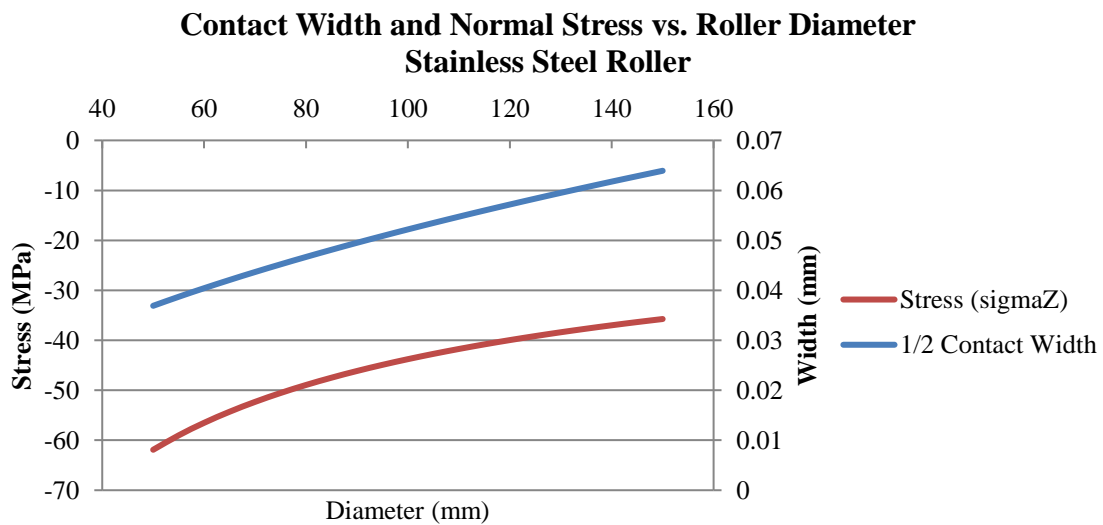


Figure 6.8 Contact Widths and Normal Stress vs. Roller Diameter

By increasing the contact width from 70 mm to 140 mm, the contact width increases from 0.08 mm to 0.12 mm. The maximum normal stress at the center of the roller decreases from -52.32 MPa to -37.00 MPa. While these changes do not appear to

be very significant, they will indeed improve consolidation as the normal stresses become less concentrated. A more in-depth analysis should be performed in order to fully determine the potential increases in feed rate and process throughput.

6.3.3 INFLUENCE OF ADDITIONAL ROLLERS ON TOW TENSION

It has already been discussed how adding the additional rollers reduces the overall compaction pressure on the material. While this alone does not actually translate to an improvement in consolidation, adding additional rollers along with a primary compaction roller does indeed improve consolidation and improve feed rate. The mechanism behind this improvement is the increase in tow tension post compaction from the primary roller.

Without the secondary rollers, unreasonable feed rates below 0.2 mm are needed for achieving very mediocre in-situ consolidation at $n = 2$ with the primary and secondary heaters set to 480 °C. The lowest tow tension is needed ($F_t = 5 N$), as the bond strength is weak and increasing the tow tension will add in-plane shear stresses that cause delamination. Adding additional rollers increases the tension to the tow post compaction, effectively increasing the dwell time and improving consolidation. In addition, increasing the length of the heated zone by adding more secondary rollers allows for the consolidated tow to cool down without a sudden release of tension and pressure. The use of a compaction shoe or track system rather than secondary rollers may provide the same benefits with a greater distribution of pressure.

The ideal compaction forces for the second layer consolidation were found and single lap shear specimens were manufactured, tested, and compared with the control specimens described in section 4.4.2. The results of these tests are listed below in table 6.4.

Table 6.4 SLS Test Results for Experiment 4

	Number of Rollers, N_r	Compaction Force, F_c (N)	Peak Load (N)	Peak Stress (N/mm^2)
1. Specimen 1	2	163	634	3.93
2. Specimen 2	2	163	649	4.02
3. Specimen 3	2	163	763	4.73
4. Specimen 4	3	226	775	4.81
5. Specimen 7	4	314	697	4.32
6. Specimen 8	4	314	571	3.54
7. Specimen 9	4	314	626	3.88

Specimens 5 and 6 had very poor bond strengths and could not be feasibly tested. It is believed that the poor consolidation was caused by movement of the heater tip which resulted in a lower temperature at the nip region. The results of these tests are compared to the results of the control specimens tested (shown in table 6.5). A total of 14 specimens were tested.

Table 6.5 SLS Test Results for Control Specimens

		Average Result	(+/-) 2 Sigma
Peak Load	N	1519	336
Tensile Strength	MPa	897	198

While the control specimens failed due to fiber fracture, the 7 SLS specimens made failed due to in-plane shear at the bonded area at an average load of 673 N. This discrepancy in bond strength when comparing the AFP specimens and the control may be

explained by some results reported by Sonmez and Hahn, where it was stated that additional consolidation occurs with subsequent passes during the next layer [3].

6.4 TOW TENSION

It was mentioned in section 6.3.3 that minimal tow tension was needed without the use of the secondary rollers. With the use of these rollers, however, tow tension was not found to influence the bond. This is due to the amount of compaction pressure used in the experimentations, where increasing the tow tension to 15 N was not detrimental. A problem does occur when starting the tow, as high tow tension causes delamination while the tow is not under pressure from both the primary and secondary rollers. It is recommended that tow tension is kept at a minimum when restarting tow placement, then increased after a short time in order to improve tow straightness. It is possible that tow tension can be maximized as a function of compaction pressure, but more experiments with a higher resolution is needed.

6.5 FEED RATE AND PLY NUMBER

It was found that the feed rate does indeed increase with the number of layers that have been consolidated. As it has been previously mentioned, feed rates of 0.5 mm/s was found to be optimal with $n = 2$. This increases up to 3.5 mm/s when performing laying-up on 7 layers ($n = 7$). This result is also reported by Sonmez and Hahn [3]. It should be noted that they recommend slowing the speed for the last layer in order to achieve a greater bond strength; however, this was not investigated in this report. The list of feed rates achieved can be seen in table 6.6 below.

Table 6.6 Results for Experiment 5

Number of layers, n		3	5	7
Feed rate, f	<i>mm/s</i>	2.5	3.0	3.5

Figure 6.9 shows an example of two layups at different speeds. As previously mentioned, the compaction pressure of 52 – 57 MPa was necessary to achieve in-situ consolidation. It is possible that the compaction pressure can be lowered when increasing the number of layers, but more experimentation and a true sensitivity analysis is needed.



Figure 6.9 Layup on 3 layers ($n = 3$) at $f = 3 \text{ mm/s}$ (left) and $f = 2.5 \text{ mm/s}$ (right)

6.6 LAMINATE MANUFACTURING CHALLENGES

With the current experimental setup, layup of the 8 layer laminate was not ideal. While process characterization was performed, identifying a window of operation that allows for the layup of the 8 layers, there are several challenges that must be addressed before a truly automated in-situ consolidation process can be used.

6.6.1 SUBSTRATE AND FIRST TWO LAYERS

When the process settings for experiment 2 were given in section 4.1.2, the number of layers upon which in-situ consolidation would take place was set to $n = 2$. When experimenting with this material, it became clear that in-situ consolidation of the TC1000 tow was not possible during the first 2 layers. With the current tool, AFP head, and heat source, a minimum of 2 layers is needed to begin in-situ consolidation.

One of the largest problems stems from the fact that large amounts of heat supplied at a very low feed rate is needed during the first few layers. In order to consolidate the material on the first layer, a suitable substrate is needed where the first layer of tows can be bonded to. This substrate must be able to temporarily bond to the tows, allowing for the laminate to be removed when the entire layup is complete. The use of raw PEI as a substrate can be used as a suitable substrate, acting as a surface that can be bonded to and become part of the structure. While this works well for the layup of the first layup, the needed heat and long dwell time the first layer is exposed to during the layup of the second layer causes the PEI substrate to severely degrade and cause irreparable damage.

During their analysis of ATL of APC-2, Sonmez and Hahn [3] reported some interesting findings that may explain the excessive dwell times needed at the lower

layers. It was reported that the slowest roller speeds were needed at the lower layers, with the maximum achievable speed at the second layer being roughly 2 mm/s. In addition, high stress concentrations were reported to be detrimental to bonding. Due to the small contact width and high normal stress concentration experienced by the material, small roller sizes were reported to decrease the achievable roller speeds. Lastly, irregular surfaces reduce the time necessary for the autohesion process to begin where polymer chains diffuse and entangle. As a result, a layup at any other orientation than [0/0] increases the overall dwell time. This concept was researched by Lee and Springer [32]. The results in this report match these results, with high compaction forces causing delamination. In addition, the analysis performed in section 6.3 show how concentrated the compaction pressures are.

6.6.2 TOW STRAIGHTNESS AND PARALLELISM

Another contributing problem to the layup of the first two layers is the width of the tow coupled with the ability to control tow straightness and parallelism. With the current experimental setup being used, parallelism of 0.5 mm can be maintained for every 20 mm. This becomes a large problem for the 1/8" wide slit tape used, where 0.5mm gaps are possible every 3 - 4 mm (depending on the ply orientation) creating a very discontinuous bond throughout the surface. In order to achieve greater coverage, a small amount of overlap would be beneficial. Again, this is difficult with the use of 1/8" tows as the amount of overlap would be quite large when compared to the tow width. The use of a wider tow would help in this regard, otherwise a more developed tow management system is needed.

6.6.3 HEATING AT THE NIP REGION

The final problem that must be addressed is in the amount of heat being applied at the nip region. With the current experimental setup, the temperature and flow rate of the heated air can be preset, but these parameters cannot be controlled in-situ. After the system is warmed up, the heated area at the nip is wide enough to consolidate up to 3 tows at once (0.375"). Since the current system is designed to feed and consolidate 1 tow, this amount of heat causes the surrounding tows to warp and possibly delaminate. This problem, coupled with challenges maintaining tow parallelism, makes in-situ consolidation of the first 2 layers extremely difficult. Figure 6.10 below shows an example these problems being coupled. The small gaps are caused by the varying tow position, the missing tows are a result of excessive heat while not under pressure causing delamination, and the waviness in the previous layer is the result of not using a substrate.

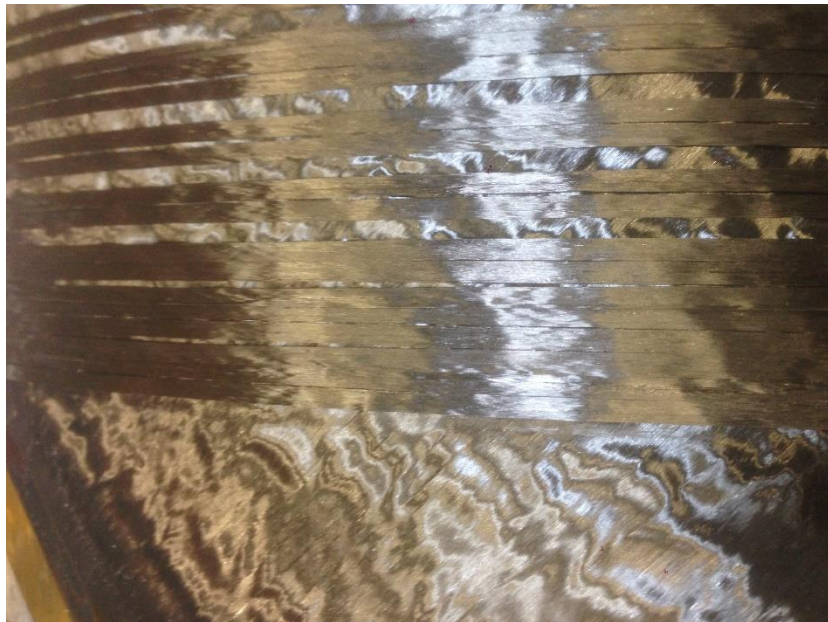


Figure 6.10 In-situ consolidation challenges during the layup of the 3rd layer

6.6.4 POTENTIAL SOLUTIONS

The most obvious solution to some of these challenges comes from improving the precision of the heat application, allowing for the exact amount of material being compacted to be heated. While hot air/gas heaters are by nature less precise than a laser heating system or an IR heater similar to what was tested in this report, there are several modifications that can be made in order to correct the problems that currently exist. Switching from this modified heater to a purpose built HA heater that can be controlled in-situ will greatly improve the precision. In addition, using a wider roller will also mitigate the problems associated with the width of the heated region at the nip region.

Using a wider tow will also help in this regard, as more of the tow will be bonded when it is first placed. As previously mentioned, using a wider tow will also aid in the layup of the first 2 layers while also greatly increasing the process throughput. Increasing the tow width used will limit any steering that will be done, however.

6.7 FIBER STEERING

With the fabrication of a working experimental AFP machine and the interaction of the process parameters investigated, fiber steering was attempted. As identifying the limits of fiber steering with thermoplastic composites is beyond the scope of this research, these trials were only performed in order to determine whether the current setup and process could be applied to the fabrication of VSC. Fiber steering at a radius of 200 mm was achieved with the 1/8" carbon/PEI slit tape and can be seen below in figure 6.11.



Figure 6.11 Fiber steering trials at a radius of 200 mm

CHAPTER 7 CONCLUSIONS

In order to investigate the interaction of process parameters necessary for in-situ consolidation of thermoplastic composites with a PEI matrix material, an experimental AFP machine was developed. In order to develop this experimental setup, different heating systems were compared and analyzed. Various experiments were then performed in order to determine the influence compaction pressure, heat application, tool temperature, and tow tension have on the lay-up. In addition, the change of these parameters as the number of layers consolidate increases was also investigated. The results from these experiments help characterize the process, and are as follows:

- Both the HA and IR heating systems can be used for in-situ consolidation of carbon/PEI slit tape in an AFP process. The HA system provides simple and effective heating that is easily controlled, however, careful positioning of the tip is needed and the heated region at the nip is significantly greater than the IR system.
- An IR heating system can be used, however, the size and position of the lens limits the design of the AFP head. If this constraint can be addressed, however, heating of the material can be performed with greater precision, at faster feed rates, and at a fraction of the cost of a laser heating system.

- The current feed rates achieved ($f = 0.5 - 3.5 \text{ mm/s}$) indicate that heating of the material at the nip region below $480 \text{ }^\circ\text{C}$ is not advisable. While material degradation for PEI has been reported to begin at around $500 \text{ }^\circ\text{C}$, no detrimental effects were seen for temperatures between $480 - 520 \text{ }^\circ\text{C}$ at the nip region. It is possible that high heating can allow for higher feed rates.
- Maintaining the appropriate compaction pressure is critical to the consolidation of the tow, with a range of $52 - 58 \text{ MPa}$ found to be acceptable. Increasing the compaction pressure results in highly concentrated normal stresses that has detrimental effects. A consolidation pressure that is too low does not promote diffusion of the polymer chains at manufacturing speeds.
- The addition of secondary rollers is very beneficial to the in-situ consolidation of the material due to an increase in tow tension between the primary and secondary roller. While the distance between both rollers is desired to be as small as possible, increasing the heated length by the addition of multiple secondary rollers may aid the process by allowing the material to cool under pressure and tension.
- Tow tension must be kept at a minimum ($\leq 5 \text{ N}$) when starting the fiber placement. When the secondary roller comes in contact with the tow, however, tow tension can be increased in order to improve tow straightness. With the use of secondary rollers, tow tension did not affect the bond strength at the range tested in this report.
- The achievable feed rates did indeed increase as a function of layer number. During the lay-up of the 8th layer, feed rates of 3.5 mm/s were achieved.
- The second iteration of this experimental setup, where further automation of the process will be implemented, should address the heat application at the nip region and

better manage the tow placement in order to manufacture a laminate. The use of wider tows is also recommended, in only for the first and last 2 layers.

- Layup of the first 2 layers was not possible. While use of wider tows will yield beneficial results, research into the substrate used and method it is applied should be performed.
- Fiber steering is possible at a radius of 200 mm when using a 1/8" tow; however, more experiments are needed to fully investigate this process.

With this information, the development of a second experimental setup where tow cutting and automated tow feeding is incorporated. If the recommended changes are adopted, large improvements in process throughput will be seen and large scale thermoplastic composite laminates can be fabricated. Lastly, research into the fabrication of thermoplastic variable stiffness composites can begin.

CHAPTER 8 FUTURE WORK AND RECOMMENDATIONS

Since a sensitivity analysis has yet to be performed, the first recommendation is that the control factors be narrowed and more concise experiments are performed. This will allow for a much greater understanding on how each process parameter can be altered in-situ or whether or not this level of control is actually needed for certain control factors. In order to perform this analysis, it is recommended that a laminate be manufactured for each trial from which a test specimen can be cut. The SLS specimens used in this report only identify the bond strength between 2 plies and the additional consolidation that occurs as a result of placement of subsequent plies is not taken into account.

As previously mentioned, the fabrication of a second experimental setup that is truly automated is required for further research. While this setup still has utility in performing additional experiments at different control factor settings, the lack of control gained by addressing the problems previously described will unnecessarily hinder progress. The development of this experimental setup was started, with the orientation of the rollers and heaters influenced by the current setup. A rendering of this second iteration of a thermoplastic AFP machine can be seen in figure 8.1 below.

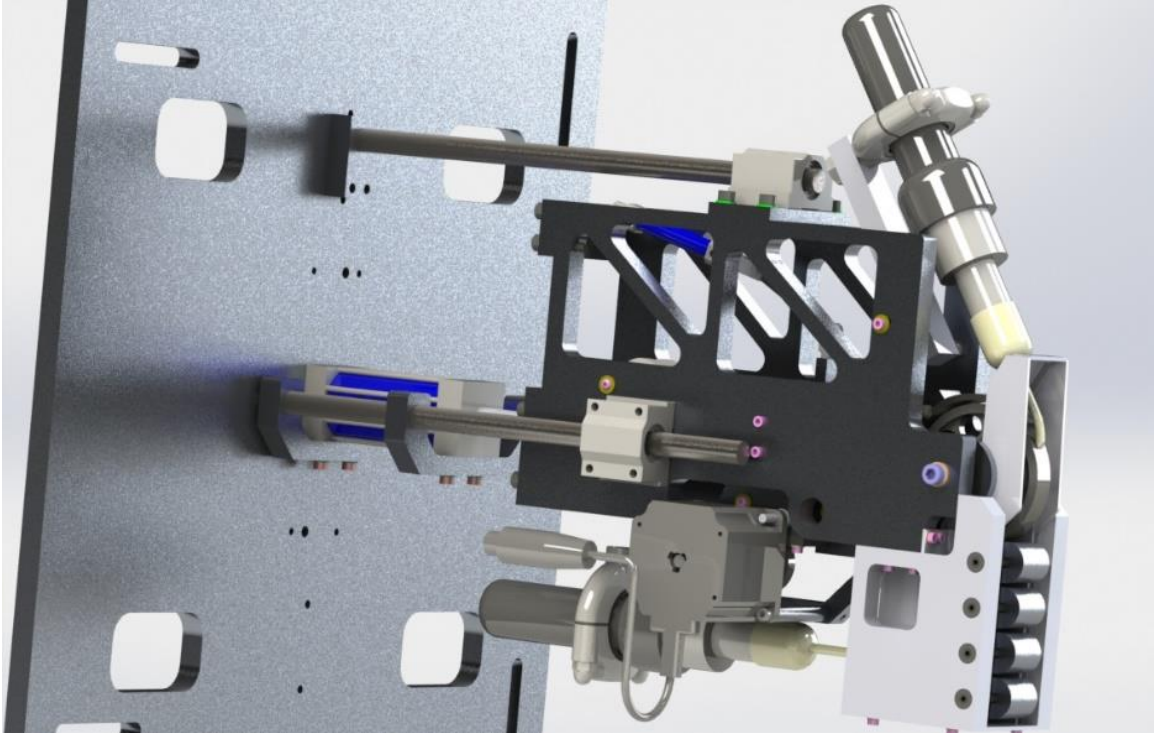


Figure 8.1 Second prototype for a thermoplastic AFP machine

Rather than using linear compression springs, this prototype utilizes a pneumatic actuator for continuously maintain a preset compaction force. In addition, tow cutting and automated tow feeding is incorporated. This design does not allow for larger compaction rollers to be used, however, and allowing for various roller diameters to be used may aid in future experimentations.

Investigation into the effect of roller diameter may be beneficial. This depends entirely on the tooling requirements, as using a roller that is too large will limit the laminate shapes that can be manufactured. By identifying the potential feed rate improvements, a true design optimization can be performed.

Investigation into additional heat sources may be beneficial. As seen in the current thermoplastic AFP industry, laser heating may yield large improvements in process throughput. Due to the costs associated with such a heating system, there may be cause to develop an AFP machine to utilize a purpose built IR heater with a double convex lens. With the current machine setup, switching to a heated gas system is feasible with minimal changes to the design. In addition, the heater orientation lends itself to swapping the HA heater wand with a laser heater if that option is investigated at a later date.

Performing fiber steering experiments are now possible and research into the minimum turn radius for various tow widths would be beneficial. This research will allow for a gap in VSC design research to be bridged by identifying manufacturing constraints. Tow straightness, surface variations at each layer, minimum turn radius, and identifying when process induced defects occur will improve the variable stiffness laminate designs.

Lastly, research into the use of additional thermoplastic matrix materials is possible. While PEEK is a commonly used thermoplastic used in various in-situ consolidation processes, slit tape with other thermoplastic matrix materials such as PPS and PEKK is also possible

REFERENCES

- [1] R. Moon, C. Johnson, and R. Hale, “Nondestructive evaluation and mechanical testing of steered fiber composites,” in *47 th International SAMPE Symposium and Exhibition 2002*, 2002, pp. 1550–1563.
- [2] K. A. P. J.A. Mondo, “Performance of In-Situ consolidated Thermoplastic Composite Structure,” *International SAMPE Technical Conference*, vol. 27, no. 361–370, 1995.
- [3] F. O. Sonmez and H. T. Hahn, “Analysis of the on-line consolidation process in thermoplastic composite tape placement,” *Journal of Thermoplastic Composite Materials*, vol. 10, no. 6, pp. 543–572, 1997.
- [4] M. Hyer and R. Charette, “Innovative design of composite structures: use of curvilinear fiber format to improve structural efficiency,” 1987.
- [5] R. Sharp, S. Holmes, and C. Woodall, “Material Selection/fabrication issues for thermoplastic fiber placement,” *Journal of Thermoplastic Composite Materials*, vol. 8, no. 1, pp. 2–14, 1995.
- [6] A. Deturk, R. Diaz, G. Digiovanni, and B. Hyman, “Exploratory tests on fiber-reinforced plates with circular holes under tension.,” *AIAA Journal*, vol. 7, no. 9, pp. 1820–1821, 1969.
- [7] H.-J. L. Dirk, C. Ward, and K. D. Potter, “The engineering aspects of automated prepreg layup: History, present and future,” *Composites Part B: Engineering*, vol. 43, no. 3, pp. 997–1009, 2012.
- [8] K. C. Wu, Z. Gürdal, and J. H. Starnes, “Structural response of compression-loaded, tow-placed, variable stiffness panels,” in *Proceedings of the 43rd Aiaa/Asme/Asce/Ahs/Asc structures, structural dynamics and materials conference, Denver, Co, 2002*, pp. 2002–1512.
- [9] W. Goldsworthy, E. Hardesty, and H. Karlson, “Geodesic path length compensator for composite-tape placement head,” 1974.
- [10] Z. Gurdal and R. Olmedo, “In-plane response of laminates with spatially varying fiber orientations-variable stiffness concept,” *AIAA journal*, vol. 31, no. 4, pp. 751–758, 1993.

- [11] A. W. Blom, C. S. Lopes, P. J. Kromwijk, Z. Gürdal, and P. P. Camanho, “A theoretical model to study the influence of tow-drop areas on the stiffness and strength of variable-stiffness laminates,” *Journal of composite materials*, 2009.
- [12] J. M. Van Campen, C. Kassapoglou, and Z. Gürdal, “Generating realistic laminate fiber angle distributions for optimal variable stiffness laminates,” *Composites Part B: Engineering*, vol. 43, no. 2, pp. 354–360, 2012.
- [13] G. Thuwis, M. Abdalla, and Z. Gürdal, “Optimization of a variable-stiffness skin for morphing high-lift devices,” *Smart materials and structures*, vol. 19, no. 12, 2010.
- [14] K. Fayazbakhsh, D. Pasini, and L. Lessard, “The effect of manufacturing parameters on the tow drop regions of a variable stiffness composite cone made out of Automated Fiber Placement,” *42nd ISTC. Salt Lake, City, UT*, 2010.
- [15] K. Croft, L. Lessard, D. Pasini, M. Hojjati, J. Chen, and A. Yousefpour, “Experimental study of the effect of automated fiber placement induced defects on performance of composite laminates,” *Composites Part A: Applied Science and Manufacturing*, vol. 42, no. 5, pp. 484–491, 2011.
- [16] K. Fayazbakhsh, M. A. Nik, D. Pasini, and L. Lessard, “Defect layer method to capture effect of gaps and overlaps in variable stiffness laminates made by automated fiber placement,” *Composite Structures*, vol. 97, pp. 245–251, 2013.
- [17] M. A. Nik, K. Fayazbakhsh, D. Pasini, and L. Lessard, “Optimization of variable stiffness composites with embedded defects induced by automated fiber placement,” *Composite Structures*, vol. 107, pp. 160–166, 2014.
- [18] B. Shirinzadeh, G. Alici, C. W. Foong, and G. Cassidy, “Fabrication process of open surfaces by robotic fibre placement,” *Robotics and Computer-Integrated Manufacturing*, vol. 20, no. 1, pp. 17–28, 2004.
- [19] P. Debout, H. Chanal, and E. Duc, “Tool path smoothing of a redundant machine: Application to Automated Fiber Placement,” *Computer-Aided Design*, vol. 43, no. 2, pp. 122–132, 2011.
- [20] M. Bruyneel and S. Zein, “A modified Fast Marching Method for defining fiber placement trajectories over meshes,” *Computers & Structures*, vol. 125, pp. 45–52, 2013.
- [21] L. Yan, Z. C. Chen, Y. Shi, and R. Mo, “An accurate approach to roller path generation for robotic fibre placement of free-form surface composites,” *Robotics and Computer-Integrated Manufacturing*, vol. 30, no. 3, pp. 277–286, 2014.

- [22] K. Tessnow, "Development of a Complex Fiber Placed Carbon/PEEK Airframe Component," in *ANNUAL FORUM PROCEEDINGS-AMERICAN HELICOPTER SOCIETY*, 1999, vol. 55, no. 1, pp. 341–355.
- [23] M. Pasanen, R. Morris, and J. Hethcock, "Manufacturing process development of a thermoplastic matrix composite horizontal stabilizer," in *AHS International, 58 th Annual Forum Proceedings-*, 2002, vol. 1, pp. 430–439.
- [24] R. J. Langone, M. Pasanen, J. Mondo, and J. Martin, "Continued development of automated, in-situ processing for thermoplastic composite structures and components," *Evolving technologies for the competitive edge*, pp. 56–64, 1997.
- [25] Z. August, G. Ostrander, J. Michasiow, and D. Hauber, "Recent developments in automated fiber placement of thermoplastic composites," *SAMPE J*, vol. 50, no. 2, pp. 30–37, 2014.
- [26] Z. A. D. H. Robert Becker P.E., "Development of Laser Heating to be used in the Processing of Thermoplastic Composites," 2012.
- [27] M. G. Nejhad, "Issues related to processability during the manufacture of thermoplastic composites using on-line consolidation techniques," *Journal of Thermoplastic Composite Materials*, vol. 6, no. 2, pp. 130–146, 1993.
- [28] S. Carroccio, C. Puglisi, and G. Montaudo, "Thermal degradation mechanisms of polyetherimide investigated by direct pyrolysis mass spectrometry," *Macromolecular Chemistry and Physics*, vol. 200, no. 10, pp. 2345–2355, 1999.
- [29] L.-H. Perng, "Thermal decomposition characteristics of poly (ether imide) by TG/MS," *Journal of Polymer Research*, vol. 7, no. 3, pp. 185–193, 2000.
- [30] A. International, "Standard test method for apparent shear strength of single-lap-joint adhesively bonded metal specimens by tension loading (metal-to-metal)," *ASTM D1002-10, ASTM International, West Conshohocken, PA, USA*, 2010.
- [31] M. Favaloro and D. Hauber, "Process and Design Considerations for the Automated Fiber Placement Process," in *ADC Acquisition Company, presented at the SAMPE 2007 fall technical conference, Cincinnati, OH*, 2007.
- [32] W. I. Lee and G. S. Springer, "A model of the manufacturing process of thermoplastic matrix composites," *Journal of composite materials*, vol. 21, no. 11, pp. 1017–1055, 1987